10

WHY DO REACTIONS HAVE ACTIVATION BARRIERS?

PRÉCIS

A knowledge of activation barriers plays a critical role in chemical kinetics. In Chapter 5, we showed that if one knows how to estimate activation barriers for a series of elementary reactions, one can predict the mechanisms of the overall reaction. In Chapters 7–9, we showed that if one knows the activation barriers and potential energy surfaces, one can predict the rate constants for each of the elementary steps in the mechanism. So far, we have assumed that we knew the potential, and have used that knowledge to make predictions.

In the next two chapters, we will concentrate on finding ways to predict activation barriers for reaction. The main focus of this chapter (10) will be to provide an overview of why chemical reactions have activation barriers. We will focus on the general models that people have proposed to estimate activation barriers for elementary chemical reactions. Some of the ideas are old. However, some of the ideas are more modern and not completely established. Most of the discussion in Chapter 10 will be qualitative. We will quantify the ideas in Chapter 11.

10.1 INTRODUCTION

The idea that reactions are activated dates back to Faraday's work in 1834. Faraday proposed that chemical reactions are not instantaneous because there was an electrical barrier to reaction. Faraday postulated that molecules were held apart by an electrical force and that one needs to overcome that force in order for reaction to happen. Faraday's ideas were proposed 75 years before people could measure an activation barrier. Consequently, Faraday never quantified his ideas. However, Faraday's ideas still were very important in the development of kinetics.

Not much progress was made in quantifying the activation barriers until Arrhenius' work appeared in 1889. Arrhenius (1889) proposed that reactions would follow

Arrhenius' law

$$\text{Rate} = \text{rate}_0 \times e^{-E_a/k_B T} \tag{10.1}$$

where rate is the rate of reaction, E_a is the activation barrier, k_B is Boltzmann's constant, T is the temperature, and rate_0 is a constant. Arrhenius also derived equation (10.1) by assuming that only hot (i.e., excited) molecules could react. According to Arrhenius, the activation barrier was associated with the energy the molecules needed to get them hot enough to react.

Later Bodenstein expanded on these ideas. Bodenstein noted that overall reactions occur via a series of elementary steps where bonds break and form. Bodenstein showed that Arrhenius' law is applicable only to elementary reactions. Overall reactions often show deviations from Arrhenius' law.

10.1.1 Models for Activation Barriers for Elementary Reactions

Over the years many models were proposed to understand why elementary chemical reactions are activated.

In 1935, Polanyi and Evans discussed the idea that bonds stretch during elementary reactions. The stretching causes a barrier. See Evans and Polanyi (1935, 1936, 1937, 1938). Bonds also break. The bond scission also causes a barrier.

More recent studies indicate that activation barriers are subtle. There are many different reasons why activation barriers arise during elementary chemical reactions, the main causes of these effects are listed in Table 10.1. Also

- Bonds need to stretch or distort during reaction. It costs energy to stretch or distort bonds. Bond stretching and distortion is one of the major causes of barriers to reaction.
- In order to get molecules close enough to react, the molecules need to overcome Pauli repulsions (i.e., electron–electron repulsions) and other steric effects. The Pauli repulsions are another major cause of barriers to reaction.
- In certain special reactions, there are quantum effects that prevent the bonds in the reactants from converting smoothly from the reactants to the products. Quantum effects can produce extra barriers to reaction.
- There are also a few special cases where the reactants need to be promoted into an excited state before a reaction can occur. The excitation energy provides an additional barrier to reaction.

For example, consider the following elementary reaction:

$$H + CH_3CH_2 \longrightarrow H_2 + C_2H_4 \tag{10.2}$$

Table 10.1 Principal causes of barriers to chemical reactions

Bond stretching and distortion
Orbital distortion due to Pauli repulsions
Quantum effects
Special reactivity of excited states

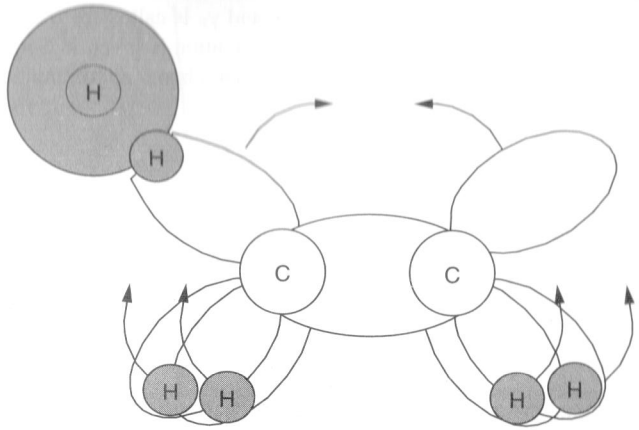

Figure 10.1 The changes in the geometry during reaction (10.2).

Figure 10.1 shows the changes in the geometry during the reaction. First the hydrogen needs to come in and get close enough to react. Then the hydrogen is transferred from a carbon atom to the hydrogen. Simultaneously, the other hydrogens flip up, the carbon–carbon bond shortens, and an orbital on each carbon rehybridizes to form a π (pi) bond. There are barriers to getting the incoming hydrogen close enough to the methyl group to react. There are barriers to the stretching of the carbon–hydrogen bond. There is a Pauli repulsion associated with the shortening of the carbon–carbon bond. There is also a quantum effect associated with the formation of the double bond. All of these effects occur simultaneously, and so it is difficult to estimate a barrier for a reaction like reaction (10.2).

One can use quantum-mechanical methods, as described in Chapter 11, to calculate the strength of the barrier. However, you do not necessarily know why the barrier arises from such calculations. Therefore, in this chapter, we will break up the problem and look at one effect at a time.

I want to say at the beginning that, while there are many theories about why barriers arise in chemical reactions, the models have not yet been completely quantified except in special cases. Consequently, while we do have many models, one still does not always know which model applies in each situation.

10.2 BARRIERS ASSOCIATED WITH BOND EXTENSIONS

In the remainder of this chapter we will discuss each of the effects in Table 10.1. To start off, we will discuss the barriers that arise because bonds need to be distorted during an elementary reaction.

The idea that bond stretching could cause barriers to reaction was first discussed by Evans and Polanyi (1935, 1936, 1937, 1938). Polanyi argued that bonds are extended during reaction, and that this phenomenon caused barriers. Polanyi had previously found empirically that barriers to reaction for similar reaction could be fit to what is now called the *Polanyi relationship*:

$$E_a = E_a^0 + \gamma_P \Delta H_r \tag{10.3}$$

where E_a^0 is called the *intrinsic activation barrier* and γ_P is called the *transfer coefficient*. Polanyi and Evans derived equation (10.3). The derivation is given in Section 10.3.

Later Marcus (1955, 1964, 1968, 1969) showed that a better approximation is given by

$$E_a = \left(1 + \frac{\Delta H_r}{4E_a^0}\right)^2 E_a^0 \tag{10.4}$$

Equations (10.3) and (10.4) are the key equations that people use to determine how bond stretching affects barriers to reaction. In the next several sections we will show how equations (10.3) and (10.4) arise, and describe when the equations work and when they fail.

10.3 DERIVATION OF THE POLANYI RELATIONSHIP

First, let us derive the Polanyi relationship, equation (10.3). The Polanyi relationship was first derived by Evans and Polanyi in 1935. At the time, there was a lot of interest in acid-catalyzed reactions. During an acid-catalyzed reaction an acid reacts with a stable species to yield products. For example, consider the acid-catalyzed reaction

$$CH_3CH_2OH \Longrightarrow C_2H_4 + H_2O \tag{10.5}$$

and assume that the reaction is taking place in aqueous solution, so that the reaction is catalyzed by hydronium ions, $[H_3O]^+$. Reaction (10.5) has been examined at great depth in the literature. The first step is a proton transfer from the hydronium to the ethanol:

$$CH_3CH_2OH + [H_3O]^+ \longrightarrow [CH_3CH_2OH_2]^+ + H_2O \tag{10.6}$$

Then the protonated ethanol loses water:

$$[CH_3CH_2OH_2]^+ + X \longrightarrow [CH_3CH_2]^+ + H_2O + X \tag{10.7}$$

Then another water reacts with the ethyl group to regenerate the hydronium:

$$H_2O + [CH_3CH_2]^+ \longrightarrow [H_3O]^+ + CH_2CH_2 \tag{10.8}$$

Evans and Polanyi assumed that in the rate-determining step of an acid-catalyzed reaction, is proton transfer from the acid to the reactant.

Next, we will derive an equation for the activation energy for the proton transfer process. We will consider the reaction $B - H + R \rightarrow B^- + HR^+$, where R is an proton acceptor, B is a conjugate base, and H is a hydrogen atom. For the purposes of derivation we will assume that one can separate the proton transfer process into two parts: the scission of the bond between the proton and its conjugate base (i.e., the negative ion produced when the proton dissociates), and the formation of a bond between the proton and the reactant to derive equation (10.3).

Figure 10.2 will be used in the derivation. Consider the transfer of a proton from an acid BH to a reactant R. We can define two quantities: r_{BH}, the length of the B–H bond; and r_{HR}, the length of the R–H bond as indicated in Figure 10.2. Following Evans and

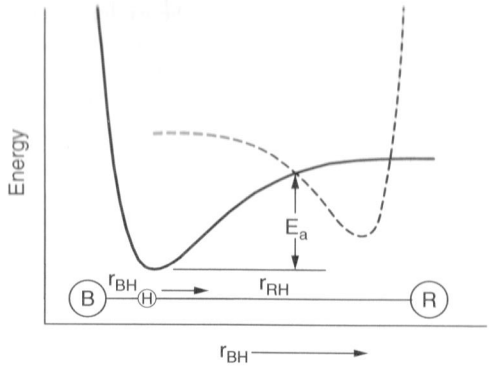

Figure 10.2 The energy changes that occur when a proton H is transferred between a conjugate base B and a reactant R. The solid line is the energy of the B–H bond; the dotted line is the energy of the H–R bond.

Polyani, we will assume that during the reaction the distance between B and R does not change. This assumption will be relaxed later in this chapter.

During the reaction, the proton–conjugate base bond breaks: r_{BH} increases while r_{RH} decreases. Figure 10.2 shows how the energy of the B–H and R–H bonds change as the reaction proceeds. The energy of a typical B–H bond looks like the solid line in Figure 10.2, where the energy of the proton increases as the proton moves from its equilibrium position. We have drawn a Morse potential, but the same arguments could be made for other potentials. The energy of the R–H bond looks similar to the potential for the B–H level. However, when we plot the data onto Figure 10.2, we need to be careful because the x axis in Figure 10.2 is the length of the B–H bond. When r_{BH} increases, r_{RH} decreases. As a result, when we plot the potential energy function of the R–H bond as a function of r_{BH}, the curve will be backwards as indicated by the dotted line in Figure 10.2.

Now consider what happens during the reaction. Initially, the B–H bond breaks, so the potential will ride up the solid contour shown in Figure 10.2. However, once the R–H bond begins to form, the potential can go back down the dotted line in Figure 10.2. During the reaction, the scission of the B–H bond occurs simultaneously with the formation of the R–H bond. Thus, in principle, the total energy should be the sum of the two curves. However, Evans and Polanyi suggested that one can obtain a reasonable approximation by assuming that the potential energy of the system went up the B–H curve as the reaction began, and then went down the R–H curve as the reaction went to completion. Evans and Polanyi also identified E_a in Figure 10.2 as the activation energy of the reaction.

Evans and Polanyi's model, although not quantitative, was quite important. It shows that one can consider a reaction as a sum of two processes: one involving bond scission and the other involving bond formation. One can then define the potential energy surface for each of the bond scission processes, and by considering the curve crossing between the two potential energy surfaces, one can get some information about rates.

The Evans–Polanyi model has had wide applicability in the physical–organic chemistry literature. As an example of the utility of the Evans–Polanyi model, consider how Figure 10.2 changes when one changes the strength of the acid by replacing one of the ligands on the acid with a different ligand. For the moment, assume that the acid dissociates more easily. By definition, when the acid strength increases, the B–H bond becomes easier to break in solution. This corresponds to an increase in the free energy of the B–H bond. The free energy could increase if either the position or the shape of the

B–H curve in Figure 10.2 changes. However, in the examples considered by Evans and Polanyi, the changes in the shape of the potential did not make enough of a difference in the free energy to make a significant change in the acid strength. Therefore, Polanyi and Evans proposed that one can get a qualitative picture of how a change in acid strength affected the reaction by simply displacing the solid curve in Figure 10.2 up or down.

Figure 10.2 shows the result of an upward displacement. Notice that as the solid curve is displaced upward, the activation energy for proton transfer goes down. For small displacements, the activation energy varies linearly with the change in the energy of the reaction.

On a more fundamental level, the Evans–Polanyi model provides an explanation of why activation energies arise in reactions. The idea is that when a reaction occurs, one bond breaks and another one forms. One can distinguish between two cases: the case in Figure 10.3, where the process is activated; and the case in Figure 10.4, where the curves cross at the minimum in the BH potential so the activation energy is zero. Fundamentally, the two cases are similar. However, when the reaction starts in Figure 10.3, the energy of the system goes up as the B–H bond is stretched, and that increase is larger than the lowering in energy due to formation of the R–H bond. As a result, the total energy of the system goes up as the reaction proceeds. That causes the reaction to be activated. In contrast, in the case in Figure 10.4, the lowering of the total energy of the system due to bond formation is larger than the energy increase due to bond scission. As a result, there is no activation barrier to reaction.

It happens that most real cases look closer to the case in Figure 10.3 than the case in Figure 10.4. Consider reaction $A + BC \rightarrow AB + C$. In the initial part of the reaction, A is moving in toward B–C. At long range, the A–BC potential is attractive, but as A gets closer, the A–BC potential is usually repulsive. The electron cloud of A overlaps with the electron cloud of B–C. That produces an electron–electron repulsion (i.e., a Pauli repulsion) of the type discussed in Chapter 9. The Pauli repulsions tend to keep the reactants from getting closer than their van der Waals radii. Now, as the reaction proceeds, the B–C bond begins to break and the A–B bond begins to form. However, the van der Waals radii of the molecules are usually larger than the covalent radii of the atoms. As a result, when atom B begins to be transferred to A, atom A is still pretty far away from B, as illustrated in Figure 10.5. As a result, the B–C bond needs to stretch before it breaks. Generally one observes about 25% bond extensions. The B–C bond loses energy as the

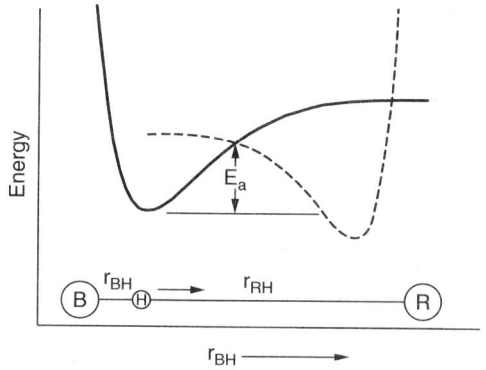

Figure 10.3 A diagram illustrating how an upward displacement of the B–H curve affects the activation energy when the B–R distance is fixed.

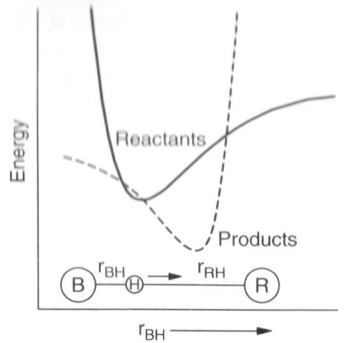

Figure 10.4 A diagram illustrating a case where the activation energy is zero.

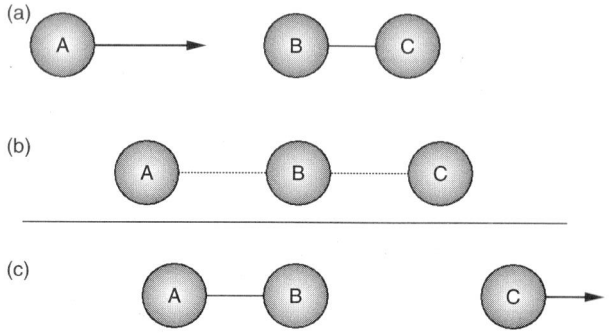

Figure 10.5 An illustration of the A–BC geometry: (a) A approaching B; (b) the transition state, (c) near the end of the reaction.

B–C bond is stretched. However, the A–B bond is still very long, so the net bonding between A and B is relatively small. This produces a situation that is analogous to the situation in Figure 10.4, where the B–C bond starts to break but the A–B bond barely starts to form. Figure 10.3 shows that in such a case, there is a finite barrier to reaction. Figures 10.3 and 10.5 apply to most reactions. As a result, most reactions are activated.

A more careful analysis indicates that activation energies can also arise because of bond distortions. However, the basic implication of the Evans–Polanyi model is that activation barriers arise because of the Pauli repulsions and because of the bond scissions and bond distortions that occur during reaction. The activation is zero only when no bonds break or distort during reaction, or when the reaction is so exothermic that bond formation dominates over bond scission. Both cases are rare. As a result, most reactions are activated.

10.4 THE POLANYI RELATIONSHIP

The analysis in the previous section was all qualitative. However, Polanyi and Evans showed that one can use the model to derive equation (10.3). In the material that follows, we will reproduce Polanyi and Evans' derivation to see how the ideas arise.

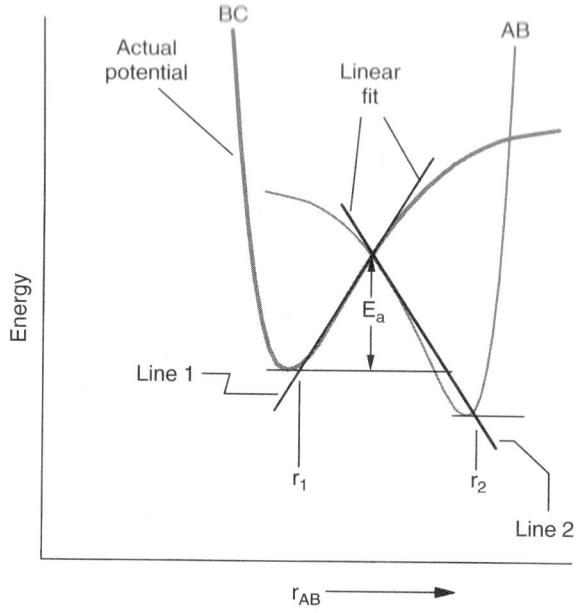

Figure 10.6 A linear approximation to the Polanyi diagram used to derive equation (10.11).

Consider the reactions $A + BC \rightarrow AB + C$. One can model the reaction as motion along the potential energy in Figure 10.12. The reactants come together at a constant value of r_{BC}, then atom B is transferred, and the reactants move away along a line of constant, r_{AB}. It is useful to consider a slice of the potential energy along the dashed line in Figure 10.12. Figure 10.6 shows how the energy varies along the slice. The horizontal axis (abscissa; x axis) in the figure is the distance along the dashed line, measured from the upper left corner of Figure 10.12. The vertical axis (ordinate; y axis) is the energy measured relative to the reactants. Notice that the potential goes up, reaches a maximum and then goes down.

Polanyi suggested that one can view the potential as being composed of a reactant potential E_1 and a product potential E_2. The two potentials are assumed to cross at the transition state.

For the purposes of derivation, it is useful to fit lines to the potential energy contour for the reaction as shown in Figure 10.6, where the lines are chosen to fit the tangent of the AB and BC potentials in the transition state. For the purposes of the derivation, it will be useful to assume that E_1 and E_2 are given by

$$E_1 = E_{reactant} + |Sl_1|(r_{ABC} - r_1) \quad \text{(reactants)} \tag{10.9}$$

$$E_2 = E_{product} + |Sl_2|(r_2 - r_{ABC}) \quad \text{(products)} \tag{10.10}$$

where $E_{reactant}$ is the reactant energy; $E_{product}$ is the product energy; E_1 is the line moving up from the reactants; E_2 is the line moving from the products; r_{ABC} is the distance along a coordinate, moving from left to right along the dashed line as in Figure 10.12; and Sl_1 and Sl_2 are the slopes of the two potential energy curves at the transition state.

Notice from Figure 10.6, E_a is equal to the energy at which line 1 intersects line 2. Solving equations (10.9) and (10.10) simultaneously for $E_a = E_1 = E_2$ and noting that $E_{product} - E_{reactant} = \Delta H_r$ yields

$$E_a = \left(\frac{|Sl_1||Sl_2|}{|Sl_1| + |Sl_2|}\right)(r_2 - r_1) + \frac{|Sl_1|}{|Sl_1| + |Sl_2|}\Delta H_r \tag{10.11}$$

Substituting

$$E_a^0 = \left(\frac{|Sl_1||Sl_2|}{|Sl_1| + |Sl_2|}\right)(r_2 - r_1) \tag{10.12}$$

$$\gamma_P = \frac{|Sl_1|}{|Sl_1| + |Sl_2|} \tag{10.13}$$

into equation (10.11) yields

$$\boxed{E_a = E_a^0 + \gamma_P \Delta H_r} \tag{10.14}$$

Equation (10.11) is called the *Polanyi relationship*. Equations (10.11) and (10.14) are the key Evans–Polanyi results. The implication of equation (10.11) is that if one had some way to change either the enthalpy or the free energy of a reaction, the activation energy for the reaction would also change. The activation barrier would also change if $|Sl_1|$ or $|Sl_2|$ were to change, or if $(r_2 - r_1)$ changed.

10.4.1 Key Predictions of the Polanyi Relationship

Physically, one can change the enthalpy of a reaction by adding a substituent group to one of the reactants. For example, consider the reaction between acetic acid and ethanol to yield ethylacetate:

$$CH_3COOH + CH_3OH \longrightarrow CH_3COOCH_3 + H_2O \tag{10.15}$$

One can vary the acid strength of the acetic acid by fluorinating the methyl group. That makes the reaction more exothermic, which in turn leads to a lowering of the activation barrier for the reaction.

Experimentally, one often finds that the activation barrier for a series of closely related reactions varies linearly with the heat of reaction. Figure 10.7 shows how the activation barriers for a number of hydrogen transfer reactions vary with the heat of reaction. Notice that in the case of hydrocarbons, there is an approximately linear relationship between the heat of reaction and the activation barrier for the reaction. Consequently, the Polanyi relationship has proved to be quite a useful way to correlate data.

Another key prediction of the Polanyi relationship is that in general strong bonds will be harder to break than weaker bonds. To see that, it is useful to compare the potentials for forming a strong bond and a weaker one. Figure 10.8 shows the plot of the potential for breaking a strong bond and breaking a weaker bond. Notice that as you increase the strength of a bond, you increase Sl_1. According to equation (10.12), if everything else is equal, that should increase the barrier to reaction.

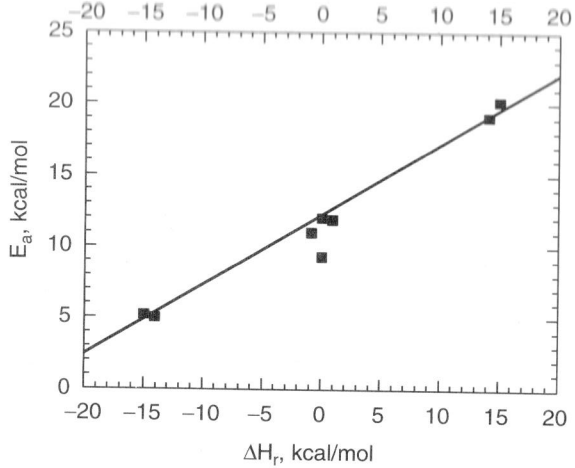

Figure 10.7 A plot of the activation barriers for the reaction $R + HR' \rightarrow RH + R'$ with R, R = H, CH_3, OH plotted as a function of the heat of reaction ΔH_r.

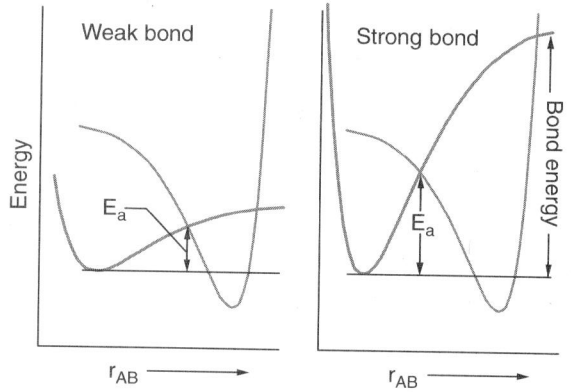

Figure 10.8 A schematic of the curve crossing during the destruction of a weak bond and a strong one for the reaction $AB + C \rightarrow A + BC$.

Another important effect is that, if everything else is equal, as you increase $(r_2 - r_1)$, the barriers to reaction increase. One calls reactions with small values of $(r_2 - r_1)$ reactions with **tight transition states**. If $(r_2 - r_1)$ is small, one does not have to stretch the bonds very much for reaction to happen. Consequently, if everything else is equal and there are no other effects, the barriers to reaction will be small.

One calls reactions with large values of $(r_2 - r_1)$, reactions with **loose transition states**. If $(r_2 - r_1)$ is large, one has to stretch the bonds a lot in order to get reaction to happen. Consequently, if everything else is equal and there are no other effects, the barriers to reaction will be large.

In actual practice, everything is rarely equal. Stronger bonds are not necessarily harder to break than weaker bonds. Reactions with looser transition states do not necessarily have

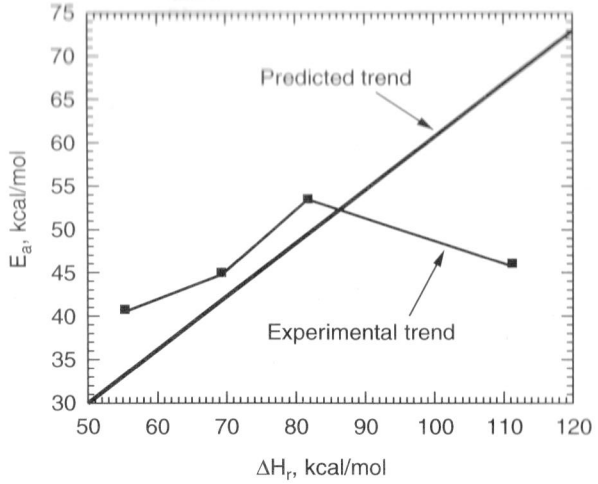

Figure 10.9 The activation barrier for the reaction $X + CH_3X \rightarrow XCH_3 + X$. The numbers are from the calculations of Glukhoutsev, et al. (1995).

larger barriers to reaction. For example, Figure 10.9 shows some data for the reaction

$$X^- + CH_3X \longrightarrow XCH_3 + X^- \qquad (10.16)$$

for $X = F^-, Cl^-, Br^-, I^-$. Notice that the activation barrier hardly changes as the strength of the CH_3X bond increases. At first, one might think that this result violates the Polanyi relationship, but actually it does not. What is happening physically is that as you change the strength of the CH_3X bond, you increase SI_1 and SI_2 but you decrease $(r_2 - r_1)$. The net effect is that the barrier to reaction is hardly changed.

Another limitation is that one needs to be careful when using the Polanyi relationship with polar and nonpolar molecules. For example, Figure 10.10 shows a plot of the activation barrier for a number of hydrogen transfer reactions of the form

$$RH + R' \longrightarrow R + HR' \qquad (10.17)$$

with R, R′ = *t*-butyl, phenyl, CCl_3, CF_3, CH_3CH_2, H, H_2N, OH, CH_3, CH_3O. Notice that although there is some correlation to ΔH, the correlation is poor. Roberts and Steele report a correlation coefficient of 0.544. This example shows the difficulty with using the Polanyi relationship for molecules with widely varying properties. In particular, polar molecules and nonpolar molecules do not belong on the same plot.

This brings up an important point—activation barriers are subtle. If everything else is equal, increasing the heat of reaction (i.e., making the reaction less exothermic) will increase the barriers to reaction. If everything else is equal, increasing the strength of the bonds that are being formed and destroyed will increase the barriers to reaction. If everything else is equal, increasing the amount of bond distortion in the transition state will increase the barrier to reaction. If everything else is equal, pulling electrons out of the transition state, which lowers the Pauli repulsions, will lower the barriers to reaction. However, everything else is rarely equal. A substituent may increase the bond strength

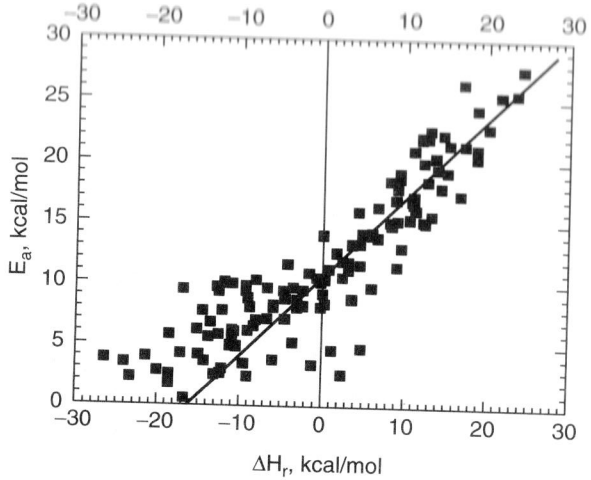

Figure 10.10 A Polanyi relationship for a series of reactions of the form $RH + R' \rightarrow R + HR'$. [Data from Roberts and Steele (1994).]

and decrease the amount of bond distortion. It is very difficult to know how the activation barrier will change in such a situation.

10.4.2 Limitations of the Polanyi Relationship

Another difficulty is that the Polanyi relationship does not work all of the time. According to the Polanyi relationship, the activation barrier for a reaction should vary linearly with the heat of reaction. Well, the linearity works, only over a limited range of ΔH_r. If one goes to a large range of ΔH_r, one finds that the Polanyi plots are generally nonlinear. Figure 10.11 shows a typical plot that one might observe in the literature. In this case one plots log(k) versus ΔH_r. Note that log(k) is proportional to $-E_a$, so according to the Polanyi relationship, the plot should be linear. However, the plot is nonlinear. The nonlinearity is typical. Consequently, the Polanyi relationship is limited to small ranges of ΔH.

Another difficulty is that the Polanyi relationships gives unphysical results for very exothermic reactions. Consider a system following the Polanyi equation:

$$E_a = 12 \text{ kcal/mol} + 0.5(\Delta H_r) \tag{10.18}$$

Notice that according to equation (10.18), a reaction with a ΔH_r more negative than -24 kcal/mol will have a negative activation barrier. That is physically impossible. Thus, the Polanyi relationship fails in the limit of very exothermic reactions.

Another physical impossibility occurs when $\Delta H_r > 24$ kcal/mol. For example, if we had a reaction with a ΔH_r of $+30$ kcal/mol, equation (10.18) would predict a barrier of 27 kcal/mol. Yet, the system must go up 30 kcal/mol to get to the products. Consequently, the activation barrier to reaction must be more than 30 kcal/mol.

One can generalize this result. In Chapter 4 we found that the activation barrier of an elementary reaction must be greater than the heat of reaction. Equation (10.18) predicts that when ΔH_r is greater that $+24$ kcal/mol, the activation barrier will be less than the heat

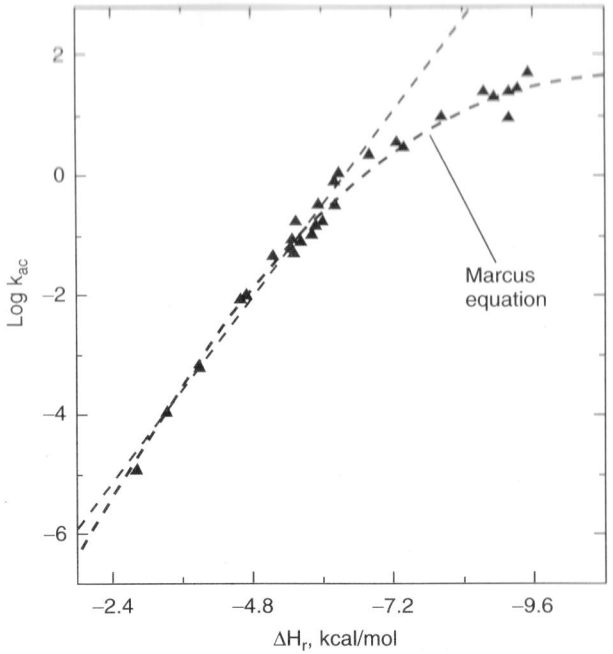

Figure 10.11 A Polanyi plot for the enolization of $NO_2(C_6H_4)O(CH_2)_2COCH_3$. Note that $\ln(k_{ac})$ is proportional to E_a. [Data of Hupke and Wu (1977).]

of reaction. Consequently, the Polanyi relationship fails in the limits of very endothermic reactions.

Generally, the Polanyi relationship is a useful approximation for reactions that are neither too endothermic nor too exothermic. However, the Polanyi relationship fails if the reactions are very endothermic or very exothermic.

10.5 THE MARCUS EQUATION

Marcus (1955, 1968) proposed an extension of the Polanyi relationship in order to overcome these difficulties with very endothermic and very exothermic reactions. Marcus considered a general reaction of the form

$$A + BC \longrightarrow AB + C \tag{10.19}$$

and derived an equation for E_a using a modification of Polanyi's methods.

In the remainder of this section, we will derive a formula for E_a using Marcus' work as a guide. Our derivation will assume that the reaction follows the solid trajectory of Figure 10.12, where the reactants come together, a reaction occurs, and then the products fly apart. We will divide the trajectory into three parts: a part where the reactants come together without being significantly distorted, a part where atom B is transferred, and a part where the reactants fly away. In this approximation, the free energy of activation is the work it takes to bring the reactants to point X, $w_r^{\ddagger}$, plus the free energy it takes to

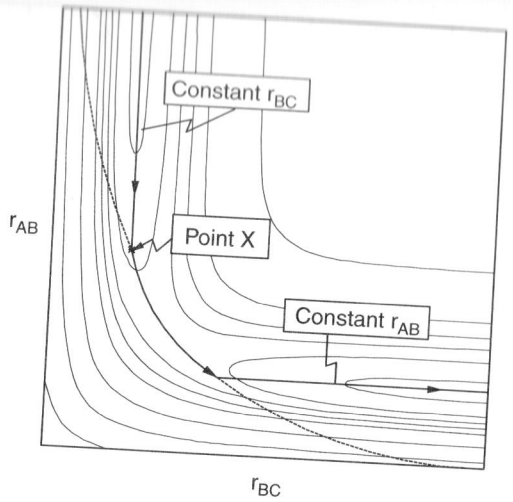

Figure 10.12 An approximation of the minimum-energy trajectory for the reaction A + BC → AB + C.

transfer atom B, E_a^1:

$$E_a = E_a^1 + w_r^1 \tag{10.20}$$

Marcus postulated with w_r^1 would be nearly constant for a group of closely related reactions, and that E_a^1 could be calculated using a modification of Polanyi's derivation described earlier in this section. For the purposes of derivation, we will define a quantity, r_X, as the distance along the dashed line in Figure 10.12 with $r_X = 0$ at point X. We will then assume that the energy of the A–B and B–C bonds follows the dotted lines in Figure 10.13 as a function of r_X where the energies show a Lennard-Jones dependence of r_X. To simplify the analysis, we will fit each of the potential contours in Figure 10.3 with a parabolic function near the transition state as indicated in Figure 10.13.

In the next few pages, we will derive Marcus' equation. For the purpose of derivation, we will assume that $E_{left}(r_X)$ and $E_{right}(r_X)$, the energies of the left and right parabolas in Figure 10.13, are given by

$$E_{left}(r_X) = SS_1(r_X - r_1)^2 + E_1 \tag{10.21}$$

$$E_{right}(r_X) = SS_2(r_X - r_2)^2 + \Delta H_r + E_2 \tag{10.22}$$

where SS_1, SS_2, r_1, and r_2 are fitting parameters. In equations (10.21) and (10.22) we have noted that E_{left} and E_{right} are functions of r_X. We will note in the material to follow that SS_1 and SS_2 are related to the vibrational frequency of the atom B as it is being transferred.

Note that since we are measuring energies from the horizontal line at the bottom of the A–B curve in Figure 10.13, E_a^1 is equal to the energy where E_{left} equals E_{right}.

For the purpose of derivation, it is useful to define $r^\dagger$ as the value of r_X where $E_{left} = E_{right}$.

From equations (10.21) and (10.22)

$$SS_1(r^\ddagger - r_1)^2 + E_1 = SS_2(r^\ddagger - r_2)^2 + E_2 + \Delta H_r \tag{10.23}$$

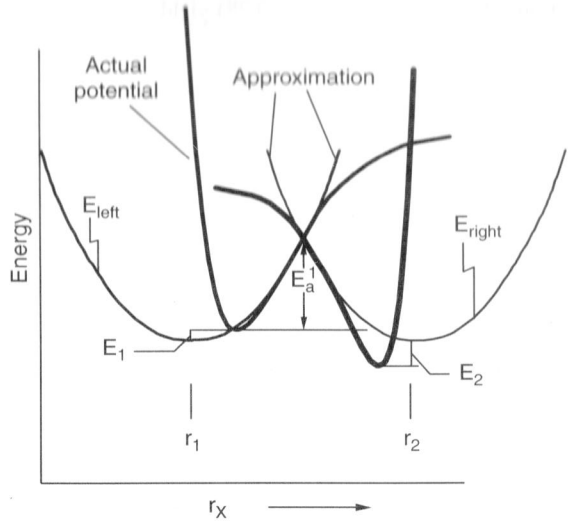

Figure 10.13 An approximation of the change in the potential energy surface that occurs when ΔH_r changes.

One can simplify equation (10.23) by assuming

$$SS_1 = SS_2 \tag{10.24}$$

$$E_2 = E_1 \tag{10.25}$$

Substituting SS_2 from equation (10.24) into equation (10.23), solving for $r^\dagger$, and then substituting E_2 from equation (10.25) yields

$$r^\ddagger = \frac{(r_1 + r_2)}{2} + \frac{E_2 - E_1 + \Delta H_r}{2SS_1(r_2 - r_1)} = \frac{r_1 + r_2}{2} + \frac{\Delta H_r}{2SS_1(r_2 - r_1)} \tag{10.26}$$

Substituting $r^\dagger$ into equation (10.21) yields

$$E_a^1 = E_{left}(r^\ddagger) = \left(\frac{r_2 + r_1}{2} - r_1 + \frac{\Delta H_r}{2SS_1(r_2 - r_1)}\right)^2 SS_1 + E_1 \tag{10.27}$$

Rearranging equation (10.27), we obtain

$$E_a^1 = \left(1 + \frac{\Delta H_r}{SS_1(r_2 - r_1)^2}\right)^2 \frac{(r_2 - r_1)^2}{4} SS_1 + E_1 \tag{10.28}$$

This equation can be put into a standard form by defining a quantity E_a^0 by

$$E_a^0 = \frac{(r_2 - r_1)^2}{4} SS_1 \tag{10.29}$$

Substituting equation (10.29) into equation (10.28) yields

$$E_a^1 = \left(1 + \frac{\Delta H_r}{4E_a^0}\right)^2 E_a^0 + E_l \tag{10.30}$$

Substituting equation (10.30) into equation (10.20) yields

$$E_a = \left(1 + \frac{\Delta H_r}{4E_a^0}\right)^2 E_a^0 + w_r \tag{10.31}$$

with

$$w_r = w_r^1 + E_l \tag{10.32}$$

People usually assume $w_r = 0$ to simplify the analysis. If $w_r = 0$, then

$$\boxed{E_a = \left(1 + \frac{\Delta H_r}{4E_a^0}\right)^2 E_a^0} \tag{10.33}$$

Equation (10.33) is called the *Marcus equation*. Marcus was awarded the 1993 Nobel Prize in Chemistry for his work on the Marcus equation and other contributions.

10.5.1 Qualitative Features of the Marcus Equation

It is useful to consider the qualitative features of the Marcus equation. Figure 10.14 shows a plot of the variation in E_a with varying ΔH_r calculated from equation (10.33) for a typical set of parameters. E_a actually varies parabolically with ΔH_r. Still, if we examine a limited range of ΔH_r, we see that E_a varies approximately linearly with ΔH_r. In contrast, when we work over an extended range of ΔH_r nonlinearities are seen. Therefore, according to the Marcus equation, one would expect reactions to obey linear free-energy relationships over a reasonable range of free energy. However, one would expect there to be some deviations from linearity if data are taken over a wide range of free energy.

Experimentally, one often finds that E_a varies linearly with ΔH_r in data taken over a limited range of ΔH_r. However, one usually observes some curvature if one takes data over a wide range of free energy. For example, consider the data in Figure 10.11. Notice that the data follow a curved line that is similar to the curved lines shown in Figure 10.14. Hupke and Wu (1977) fit the data in Figure 10.11 to equation (10.33); the results are given in Figure 10.11. Notice that the fit is good. Hence, we can explain the curvature in Figure 10.11 using the Marcus equation.

Marcus has shown that one can predict the fitting parameters in his equation from first principles, and fit real data. Further, it has been found that all of the examples in the literature that show curved free-energy plots can be explained via the Marcus formalism except those that show a change in mechanism with changing ΔH_r. Hence, the Marcus equation is quite useful in explaining data.

There is one unusual prediction of the Marcus equation. Notice that according to equation (10.33), the rate of reaction should reach a maximum (i.e., E_a should reach a

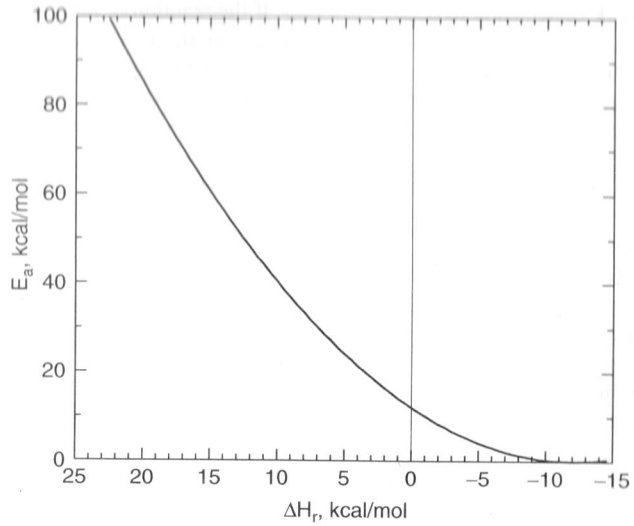

Figure 10.14 A plot of the activation barrier predicted from the Marcus equation with $E_a^0 = 12$ kcal/mol.

minimum) when $\Delta H_r = \Delta H_r^{max}$ where ΔH_r^{max} satisfies

$$1 + \frac{\Delta H_r^{max}}{8E_a^0} = 0 \tag{10.34}$$

The rate should decrease with increasing $-\Delta H_r$ when $-\Delta H_r \geq E_a^0$.

Figure 10.15 illustrates why the maximum occurs. Most reactions show Polanyi diagrams like those in Figure 10.15a, where a reaction needs to go up a potential energy

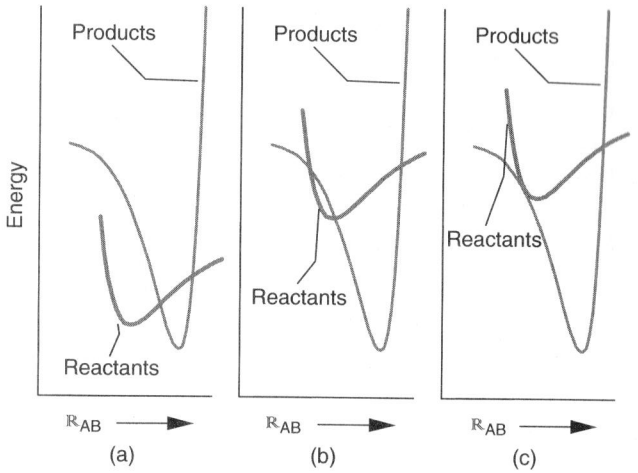

Figure 10.15 A Polanyi diagram illustrating how changes in ΔH for the reaction change the barriers to the reaction AB + C → AB + C: (a) normal case; (b) saturation; (c) Marcus inverted region.

contour and back down again to occur. However, if the reaction is sufficiently exothermic, one can get to a situation where the energy curves for the reactants and products cross at the equilibrium point for the reactants as illustrated in Figure 10.15b. Notice that at this particular potential, the activation barrier is zero. Now consider what happens when the reaction becomes more exothermic as illustrated in Figure 10.15c. Note that as we continue to increase the potential, the intersection of the energy curves for the reactants and products moves to the left, causing the activation energy for the reaction to increase.

We call the region where the rate decreases with increasing driving force the **Marcus inverted region**. Up until 1980, no one had observed Marcus inverted behavior. However, a number of electron transfer reactions that show inverted behavior have been discovered since 1980. See W. H. Miller (1991) for details. There is a complication in electron transfer reactions in that the rate of the reaction is moderated by something called a *Frank–Condon factor*, which can decrease with increasing $-\Delta H_r$. We will discuss this effect later in this chapter. At present, the best available information is that Frank–Condon factors are quite important in the **Marcus inverted region**. As a result, one cannot explain the data with the Marcus equation alone. Still, the Marcus equation gives the correct qualitative behavior even in the inverted region, and so it is quite powerful.

10.5.2 Strengths of the Marcus Formulation

One of the major strengths of the Marcus formulation is that it eliminates the difficulties of the Polanyi relationship for very exothermic and very endothermic reactions. Figure 10.16 is a plot of the height of the barrier as a function of the heat of reaction. A plot of $E_a = \Delta H_r$ is also shown in the figure. Notice that the barriers are never negative. Further, the barriers are always greater than the heat of reaction. Consequently, unlike the Polanyi relationship, the Marcus equation never gives a physically impossible result.

Another strength of the Marcus equation is that it allows the activation barrier to vary nonlinearly with the heat of reaction. For example, Figure 10.11 showed some data where the activation barrier varies nonlinearly with the heat of reaction. Figure 10.11 shows a fit of the data to the Marcus equation. Notice that the equation fits very well.

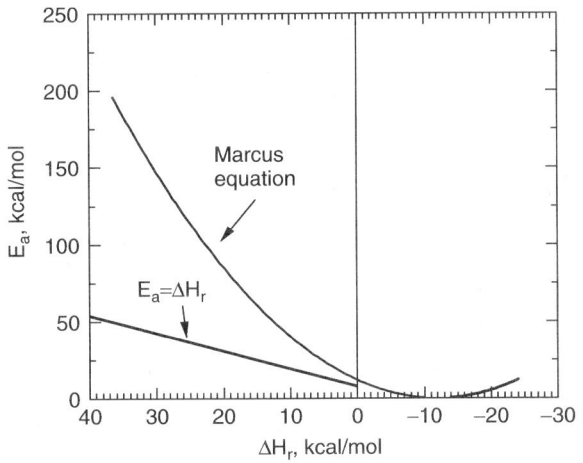

Figure 10.16 A plot of the activation barrier calculated from the Marcus equation as a function of the heat of reaction for a reaction with an intrinsic barrier of 12 kcal/mol.

One subtlety in all of this is that Cohen and Marcus (1968) have shown that E_a^0 is not constant. Rather, E_A^0 can vary over a series of reactions. That can produce complex behavior.

Fortunately, Marcus has shown that one can often estimate E_a^0 from something called 'identity reactions'. A simple calculation is shown in Example 10.A. Generally the Marcus equation allows one to estimate activation barriers from first principles. Again an example calculation is shown in Example 10.A.

10.5.3 Weaknesses of the Marcus Equation

Unfortunately, there are many examples where the Marcus equation does not fit as well (see Figures 10.17 and 10.18). Generally failures occur when you consider data taken over a wide range of ΔH_r. Figure 10.18 shows some data for some electron transfer reactions

$$R^* + CH_3CN \longrightarrow R^+ + CH_3CN^- \tag{10.35}$$

where R^*, an excited species, is deexcited via electron transfer to acetonytrile. Figure 10.17 shows data for intramolecular electron transfer processes across a spacer molecule:

$$R^- - Sp - R^+ \longrightarrow R^+Sp - R^- \tag{10.36}$$

In the first case the activation barrier reaches a maximum and then levels off. In the second case the activation barrier reaches a maximum and then decreases again. However, the decrease is much smaller than that predicted from the Marcus equation. Both of these cases show that while the Marcus equation eliminates the difficulties with the Polanyi

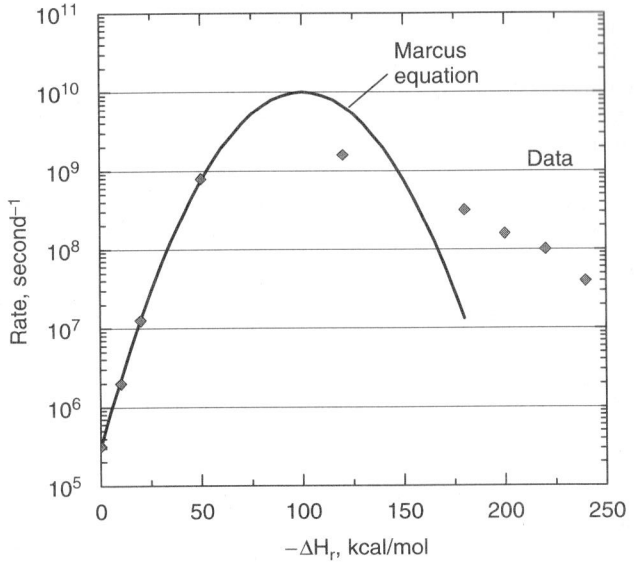

Figure 10.17 The rate of intramolecular electron transfer across a spacer molecule plotted as a function of the heat of reaction. [Data of J. R. Miller et al., (1984)].

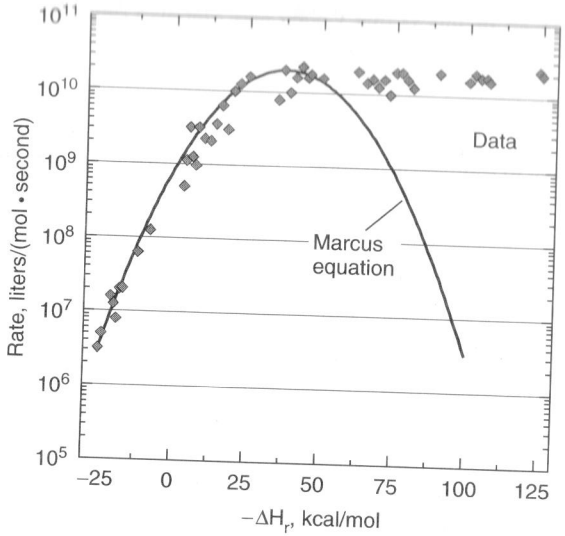

Figure 10.18 The rate of florescence quenching of a series of molecules in acetonitrite plotted as a function of the heat of reaction. [Data of Rehm and Weller (1970).]

relationship for very exothermic reactions, the Marcus equation does not entirely eliminate the difficulties.

Another weakness of the Marcus equation is that one cannot easily explain the trends in Figures 10.9 and 10.10 with the Marcus equation unless one assumes that E_a^0 varies over the series of reactions. The Marcus equation is basically a curve-crossing model. As one increases the strength of the bonds, one increases the slopes of the all of the lines, so that the barriers to reaction should increase. However, in Figure 10.9 we find that the activation barrier is not increasing substantially when one makes some substantial changes in the bond strength. People have fit the data in Figures 10.9 and 10.10 by assuming that E_a^0 varies over the series of reactions. However, if E_a^0 is treated as a variable, the Marcus equation loses its predictive power. Further, the variations in E_a^0 have not been physically reasonable.

The Marcus equation does not give the correct result for the data in Figures 10.17 and 10.18 because those figures assume that E_a^0 is constant in the series of reactions. According to the derivation of the Marcus equation in Section 10.5, E_a^0 is constant only when $(r_2 - r_1)$ in equation (10.29) is constant. In practice, $(r_2 - r_1)$ can change during reaction. Notice that according to equation (10.29), if we change $(r_2 - r_1)$, we change the barrier to reaction; when $(r_2 - r_1)$ increases, the barriers to reaction increase.

The Marcus equation gives a different result. According to the Marcus equation, when we decrease $(r_2 - r_1)$, we first decrease the barriers to reaction, and then increase them again.

The reason why the data in Figure 10.9 do not show an increase in the barrier to reaction is that $(r_2 - r_1)$ is increasing as slopes Sl_1 and Sl_2 are decreasing. The net result is that the barriers do not change.

The data in Figure 10.17 is more complicated. The Marcus equation works in the normal region for the data in Figure 10.17; however, the method fails in the Marcus inverted region. Physically, the situation is as illustrated in Figure 10.19. If one assumes

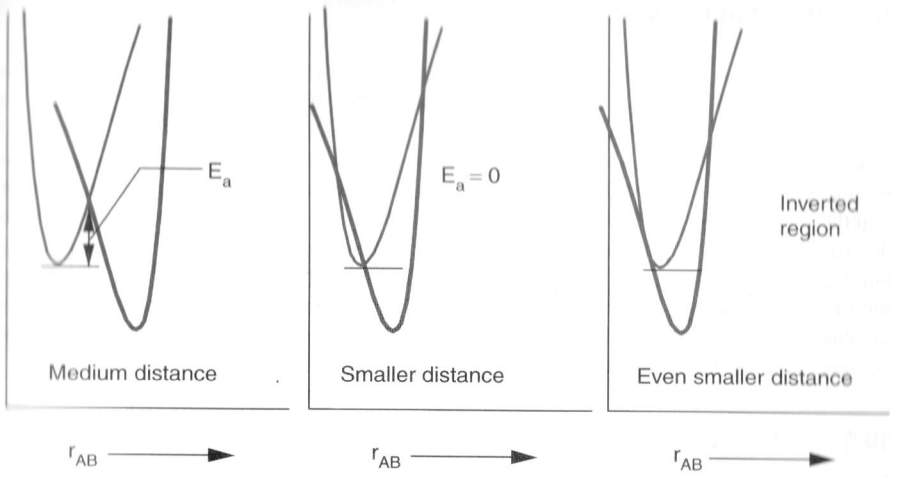

Figure 10.19 Changes in the curve-crossing model as $(r_2 - r_1)$ decreases during the reaction $AB + C \rightarrow A + BC$.

that the $(r_2 - r_1)$ is constant during the reaction, then the situation will be as seen on the right of Figure 10.19. The curves will cross in the inverted region, so the barriers to reaction should increase as ΔH becomes more negative. Note, however, that during a bimolecular reaction, $(r_2 - r_1)$ decreases as the reactants come together. Before the system gets to the situation on the right of Figure 10.19, the system will get to the situation in the middle of Figure 10.19, where the barrier to reaction is zero. Thus the barrier to reaction will be zero even though there will be a barrier at smaller values of $(r_2 - r_1)$. The derivation of the Marcus equation ignores this possibility, so it does not fit the data in Figure 10.17.

The situation in the data in Figure 10.18 is even more complex. This is a special reaction where one is transferring an electron across a molecule. $(r_2 - r_1)$ is constrained, so one cannot reach the situation in the center of Figure 10.19. As a result, one does observe an inverted region. One does not follow the Marcus equation exactly, however, because $(r_2 - r_1)$ still varies to compensate for the inverted region.

Generally one finds that the Marcus equation works well when $(r_2 - r_1)$ is constrained. If one considers a unimolecular reaction such as:

(10.37)

$(r_2 - r_1)$ represents the carbon–carbon bond length. The carbon–carbon bond length does not change significantly during reaction, so it is reasonable to assume that $(r_2 - r_1)$ is constant in such a situation. However, if one looks at a bimolecular reaction such as:

$$H + CH_3CH_2R \longrightarrow CH_4 + CH_2R \qquad (10.38)$$

$(r_2 - r_1)$ changes as one changes the heat of reaction. The Marcus equation does less well in this situation.

10.6 PAULI REPULSIONS

In order to develop a better model for the energy at the transition state, one needs to be able to predict $(r_2 - r_1)$ at the transition state. Recall from Chapter 8 that during a bimolecular reaction there are repulsions that push the reactants apart. These are called *Pauli repulsions*. As the Pauli repulsions get stronger, the reactants are pushed apart so that $(r_2 - r_1)$ increases. If the Pauli repulsions weaken, the reactants can get closer together so that $(r_2 - r_1)$ decreases. As a result, the Pauli repulsions play a key role in determining $(r_2 - r_1)$. The bond energies also play a key role. If you are forming a strong bond during the reaction, the strong bond tends to pull the reactants together. As a result, the transition state gets tighter; specifically, $(r_2 - r_1)$ decreases. In contrast, weaker bonds increase $(r_2 - r_1)$. In general, $(r_2 - r_1)$ is determined by a balance between the bond energies and the Pauli repulsions.

10.6.1 The Origin of Pauli Repulsions

In order to model $(r_2 - r_1)$, one needs to understand Pauli repulsions. Pauli repulsions are basically electron–electron repulsions. Recall from freshman physics that electrons repel each others via a Coulomb force. The Coulomb force occurs with electrons on molecules in the same way that the Coulomb force occurs when there are two isolated electrons. As a result, when two reactant molecules come together, the electrons on one reactant molecule repel the electrons on the other reactant molecule. That can produce a barrier to reaction.

The actual interaction is more subtle than it would appear from the previous paragraph. Recall that when two hydrogen atoms come together, the electrons do not repel. Instead, the electrons on the two hydrogen atoms pair up to form a bond. In Chapter 11 we will show that, because of a quantum effect called *exchange*, the electron–electron repulsion will go to zero when two electrons pair up into a bond. As a result, the electron–electron repulsion is subtler that it would first appear.

Now consider the reaction

$$D + H_2 \longrightarrow DH + H \tag{10.39}$$

The incoming deuterium can form a bond with the hydrogen, so there is an attractive interaction. Yet, the H_3 complex is not stable; that is, there is no stable H_3 molecule. Consequently, there must also be a repulsive interaction to drive the H_3 apart. This repulsion is called a **Pauli repulsion**. Note that the Pauli repulsion is more complex than a simple Coulomb repulsion because it goes to zero when the electrons in a molecule pair up to form a bond.

10.6.2 A Physical Picture of the Pauli Repulsions

One needs to use quantum mechanics to derive an exact expression for the Pauli repulsions. However, it is easy to get a graphical picture of the interactions. In the text that follows, we will describe a qualitative method that one can use to understand the interactions. The ideas will come out of molecular orbital (MO) theory. When I teach this material, I usually review MO theory. The notes from my review are in Chapter 11. Consider the reaction

$$D + H_2 \longrightarrow DH + H \tag{10.40}$$

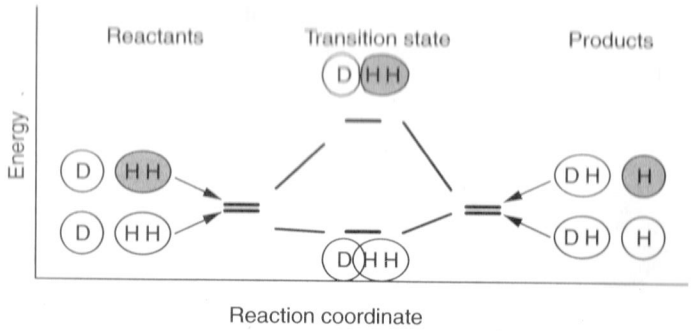

Figure 10.20 A diagram of the key molecular orbitals for the reaction $D + H_2 \rightarrow DH + H$.

The deuterium starts out with an electron in a 1s orbital while the H_2 starts out with two electrons in a σ orbital. The 1s orbital is spherical as indicated in Figure 10.20. The σ orbital starts out almost spherical, but I have drawn it more elliptical to make the diagram clearer.

When the 1s orbital interacts with the σ orbital, there are two possible molecular orbitals MOs of the system: a bonding MO where the wavefunction on the deuterium has the same sign as the wavefunction on the H_2, and an antibonding MO where the wavefunction on the deuterium has the opposite sign as the wavefunction on the H_2. In Figure 10.20 I have arbitrarily assigned a positive sign to the orbital on the deuterium and have then let the orbital on the H_2 have either a positive or a negative sign. In order to make the figure easy to see, I have made the positive orbitals light-colored and the negative orbitals dark-colored.

A key thing to remember from diagrams like this is that the light-colored orbitals attract other light-colored orbitals, dark-colored orbitals attract dark-colored orbitals, but dark-colored orbitals repel light-colored orbitals provided the orbitals are occupied.

Now consider what happens as the deuterium approaches the H_2. In the bonding state of the transition state (i.e., the bottom state in Figure 10.20), the orbitals are all of the same sign. Orbitals of the same sign attract. Therefore there is an attractive interaction between the deuterium and the H_2. In contrast, in the top state, the orbitals are of different signs. Orbitals of different signs repel. The repulsion causes the orbitals of different signs to be distorted. The distortion produces a barrier to reaction.

Another way to view this is that there is a bonding (attractive) interaction when two orbitals come together with the same sign and an antibonding interaction when two orbitals come together with different signs. For future reference we will call the former case the **bonding state** of the system, and the latter case the **antibonding state** of the system.

A subtlety is that there is always an antibonding state in the system even when there is no barrier to reaction. Physically, one gets a barrier only when the antibonding state is occupied. If all of the antibonding states are empty, there will be no electron–electron repulsions, and therefore no barriers.

We need to keep track of the electron count to see if the antibonding state is occupied. There are three electrons in the transition state for reaction (10.40). We can put two electrons in the bonding molecular orbital, so we have a two-electron attraction. However, quantum-mechanically, one can put at most two electrons into a molecular orbital. The third electron must go into the antibonding orbital. That produces a one-electron repulsion.

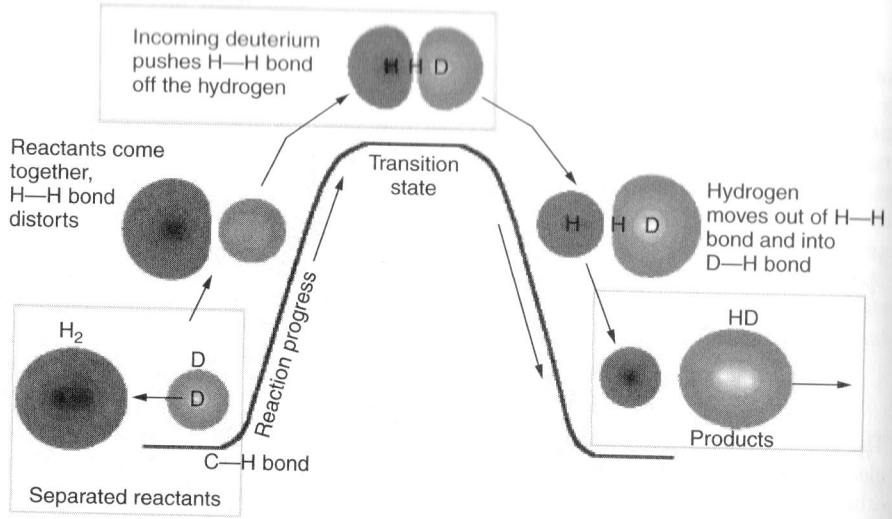

Figure 10.21 A diagram of the orbital distortions during the reaction $D + H_2 \rightarrow DH + H$.

Detailed calculations show that the attraction is 93 kcal/mol while the repulsion is 103 kcal/mol. That produces a net barrier of 10 kcal/mol.

Figure 10.21 shows a detailed picture of the orbital distortions. Notice that the orbitals distort during reaction. I like to think of the orbitals as balloons. When the deuterium comes in, it pushes the hydrogen–hydrogen bond out of the way. That allows the hydrogen atom on the left of the H_2 to be transferred to the deuterium. In this particular case, the left hydrogen is at the node between the two orbitals at the transition state for the reaction. In other reactions, we have found that the transition state can be slightly earlier or later than the point at which the hydrogen is transferred. However, one usually sees orbitals pushing into one another during reactions.

Quantum-mechanically, exothermic reactions have finite activation barriers only when filled orbitals of different signs push into one another, causing orbital distortions. If there are no orbital distortions, an exothermic reaction will not be activated. An endothermic reaction will still be activated because the system has to go uphill to get to products.

Next, let's consider a slightly different reaction:

$$D + [H_2]^+ \longrightarrow [DH_2]^+ \tag{10.41}$$

The MO diagram for reaction (10.41) is the same as that for reaction (10.40). However, there is an important difference. There are only two electrons in the transition state for reaction (10.41). One can put both electrons into the bonding state. The antibonding state is empty. Consequently, there is no barrier to reaction (10.41). There is a barrier to the following reaction, however

$$D + [H_2]^+ \longrightarrow [DH_2]^+ \longrightarrow [DH]^+ + H \tag{10.42}$$

There is no barrier to forming $[DH_2]^+$, but $[DH_2]^+$ is a stable molecule. It costs energy to break the $[DH_2]^+$ apart. Consequently, there is a barrier to reaction (10.42).

One can generalize these results to any reaction. Pauli repulsions cause barriers to reactions. The barriers arise when orbitals of different signs push up against one another. If all of the atomic orbitals have the same sign, there will be little or no barrier. Molecules would rather form MOs where all of the individual atomic orbitals have the same sign. Unfortunately, the MO with all of the atomic orbitals of the same sign can hold only two electrons. If there are three or more electrons in the system, there will be an antibonding interaction. Consequently, there will be a barrier to reaction.

10.6.3 Qualitative Picture of the Role of Pauli Repulsions on the Barriers to Reaction

Next, we want to discuss how to quantify these effects. To start off, it is important to note that at present it is very difficult to predict the strength of the Pauli repulsions exactly. Generally, one needs to do quantum-mechanical calculations, and then do analysis to estimate the strength of the Pauli repulsions. So far such calculations have been done for only a few special cases, so there is not much to say. Still, we do have pictures. I think that the pictures are important enough that I want to include them.

Figure 10.22 shows a diagram of the orbital distortions during the reaction

$$H + CH_3CH_3 \longrightarrow H_2 + CH_2CH_3 \tag{10.43}$$

This case is very much like the case in Figure 10.21. The hydrogen comes in and pushes the orbital off one of the methyl hydrogens. Again, the orbitals look like balloons pushing into one another. Lee and Masel (1996,1997) showed that the orbital distortion causes there to be a barrier to reaction.

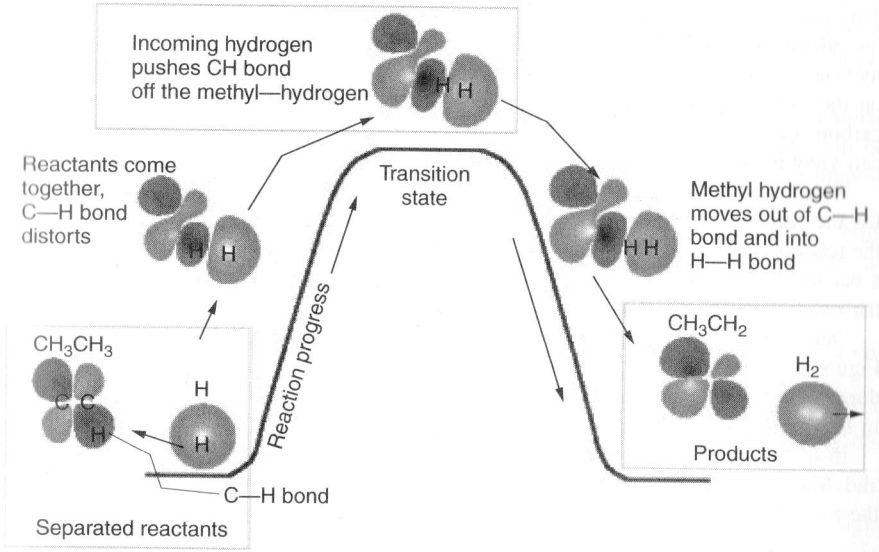

Figure 10.22 A diagram of the orbital distortions during the reaction $H + CH_3CH_3 \rightarrow H_2 + CH_2CH_3$. The diagram shows only the interaction with the E state of ethane (the C–H bond). Other MOs of the ethane also distort.

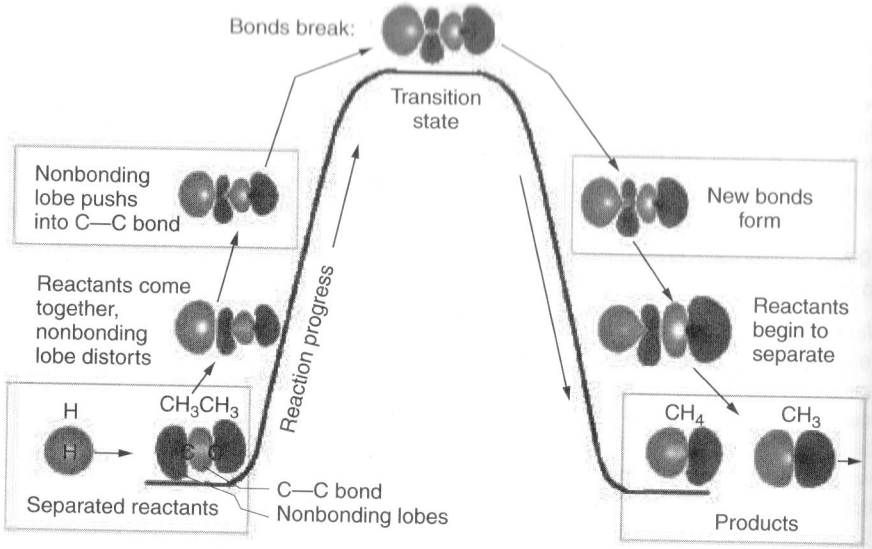

Figure 10.23 A diagram of the orbital distortions during the reaction $H + CH_3CH_3 \rightarrow CH_4 + CH_3$. Only the $3A_{1g}$ state of ethane (the state for the carbon–carbon bond) is shown.

Figure 10.23 shows a diagram of the orbital distortions during the reaction

$$H + CH_3CH_3 \longrightarrow CH_4 + CH_3 \tag{10.44}$$

This case is more complicated. The hydrogen starts out with a spherical orbital, while the ethane starts out with a carbon–carbon bond, and two nonbonding lobes. When the hydrogen collides with the ethane, the hydrogen orbital pushes into the nonbonding orbital on the methyl group. The nonbonding orbital on the methyl group then pushes into the carbon–carbon bond. The net effect is that the carbon–carbon bond breaks. Again, one can view the process as balloons pushing into one another, causing bonds to break.

Notice that the orbital distortions are much larger for the reaction in Figure 10.23 than for the reaction in Figure 10.22. The result is that the barriers to reaction are larger for the reaction in Figure 10.23 than for the reaction in Figure 10.22. Lee and Masel estimate a barrier of 10 kcal/mol for the reaction in Figure 10.22 and a barrier of 42 kcal/mol for the reaction in Figure 10.23.

One of the questions in the literature is whether the large barrier to the reaction in Figure 10.23 is caused by the Pauli repulsions or by the fact that bonds need to be distorted during reaction. Notice that you are moving hydrogens out of the way during the reaction in Figure 10.23. Those displacements could be responsible for the barriers to reaction.

In order to separate the effects of bond distortion and orbital displacements, Blowers and Masel (1999a,b) calculated the activation barriers for a number of reactions of the form

$$CH_3OH + H \longrightarrow \text{products} \tag{10.45}$$

Figure 10.24 compares the activation barriers to the bond distortion energies and the orbital distortion energies. Notice that the activation barriers increase as the orbital

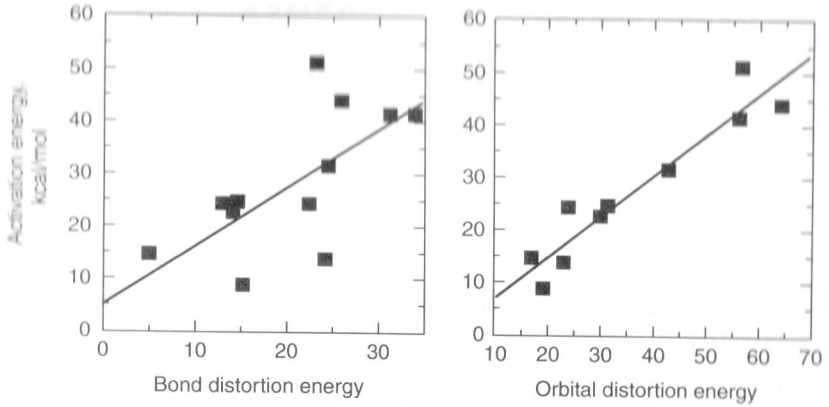

Figure 10.24 A plot of the activation energy for a number of reactions versus the bond distortion and the orbital distortion energy results of Blowers and Masel (1999a,b).

distortion energies increase. There is an excellent correlation between the barriers and the orbital distortion energies. In contrast, there is only a poor correlation between the activation energies and the bond distortion energies. Therefore, it seems that orbital distortions are more important than bond distortions in determining the barriers to reaction.

One should not infer, from the last paragraph, that bond displacements do not produce barriers. That is not true. Instead, bond distortions and orbital distortions are intimately connected. You get orbital distortions whenever you get bond distortions so that the orbital distortion energy contains a component due to the bond distortion energy. However, the orbital distortion energy has other components; one can get orbital distortions without bending or stretching any bonds. Those orbital distortions are important: more important, in fact, than the bond distortions. Consequently, the orbital distortion energy has a larger influence on the barriers than does the bond distortion energy.

In your organic chemistry class, you learned about orbital distortions in terms of **steric effects**. If you have a large group blocking a site, the reaction rate at that site will be reduced. Steric effects are important to a wide range of reactions, as you learned in organic chemistry.

Still, it is important to realize that steric effects are really manifestations of Pauli repulsions and apply only to situations where Pauli repulsions are important. Consider the following reaction:

$$[(CH_3)_2CH(NO_2)] + H \longrightarrow [(CH_3)_2C(NO_2)] + H_2 \tag{10.46}$$

The carbon atom in reaction (10.46) is blocked by a methyl group, and so the reaction rate is slow. Kresge (1974) estimates a barrier of 19 kcal/mol. However, if you change the reaction slightly

$$[(CH_3)_2CH(NO_2)] + H^+ \longrightarrow [(CH_3)_2C(NO_2)]^+ + H_2 \tag{10.47}$$

the reaction is unactivated. Physically, during reaction (10.46) the incoming hydrogen needs to overcome a large Pauli repulsion (i.e., electron–electron repulsion) in order to get the reaction to occur. In contrast, in reaction (10.47), a proton, rather than a hydrogen,

comes in. The proton does not contain any electrons, and you need electrons to get Pauli repulsions. Consequently, there are no Pauli repulsions in reaction (10.47). The absence of Pauli repulsions makes reaction (10.47) unactivated even though reaction (10.46) has a barrier of 19 kcal/mol.

There is one other case where Pauli repulsions disappear: a case where an electron is transferred at long distances. Consider the reaction

$$H + F_2 \longrightarrow HF + F \tag{10.48}$$

One might think that there is a Pauli repulsion in reaction (10.48). After all, there are electrons on the hydrogen and the F_2 that can repel. However, in practice, the hydrogen transfers an electron to the fluorine at long distances, producing H^+ and $[F_2]^-$. The electron transfer eliminates the Pauli repulsions. Consequently, reaction (10.48) is unactivated.

10.6.4 Empirical Extensions of the Polanyi Relation

In the literature, it has been common to account for the effects discussed in Sections 10.6.2–10.6.4 by empirically extending the Polanyi relationship. For example, Roberts and Steele examined a series of reaction of the form

$$BH + R \longrightarrow B + HR \tag{10.49}$$

where B is a conjugate base and R is a different conjugate base. Roberts and Steele found that the activation barriers for exothermic reactions of the form in equation (10.49) could be fit by the equation

$$E_a = E_a^O \left(\frac{H_{BH} H_{RH}}{(H_{HH})^2} \right) + \gamma_P \Delta H + \gamma_X (\chi_B - \chi_R) + \gamma_s (s_B + s_r) \tag{10.50}$$

where H_{BH} and H_{RH} are the strengths of the BH and RH bonds, H_{HH} is a normalization factor (the strength of an HH bond), γ_p is the transfer coefficient, χ_B and χ_p are the Mullikin electronegativities of B and R, s_B and s_r are structure factors fit to the data, and E_a^O, γ_X and γ_s are constants.

Physically, the first term on the right of equation (10.50) is the intrinsic barrier multiplied by a correction factor to account for the fact that stronger bonds are harder to break than are weaker bonds. The second term is the standard transfer coefficient times heat of reactions as discussed in Section 10.3. The third term is a constant times the difference in electronegativity of the two species. Physically, when the two species have very different electronegativities, there is partial charge transfer, which lowers the Pauli repulsions. The last term in equation (10.50) accounts for the fact that larger groups can have larger Pauli repulsions.

At this point, equations like (10.50) have not been derived theoretically. In fact, up until the late 1990s, people did not know why they worked. As a result, the equations are not highly respected in the literature. Still, they work very well.

One other unexplained feature at present is that the γ_p values are different for exothermic and endothermic reactions. γ_p is usually about 0.3 for exothermic reactions and about 0.7 for endothermic reactions. That has not yet been explained.

10.7 A MODEL FOR THE ROLE OF PAULI REPULSIONS ON THE BARRIERS TO REACTION

One can get some insight into equation (10.50), by developing a model to estimate $(r_2 - r_1)$ and then plugging that result into the Marcus equation. Blowers and Masel derived an equation to estimate $(r_2 - r_1)$. The idea in the Blowers–Masel model is to calculate E_a by explicitly considering how Pauli repulsions affect $(r_2 - r_1)$. Let's consider the reaction

$$H + CH_3CH_3 \longrightarrow CH_4 + CH_3 \tag{10.51}$$

We discussed the qualitative features of potential energy surfaces for reactions in Sections 8.4.2, 8.4.3, and 8.5. During reaction (10.51), a carbon–carbon bond breaks and a carbon–hydrogen bond forms. According to the analysis in Sections 8.4.2, 8.4.3, and 8.5, respectively, one can approximate the potential energy surface for the system as the sum of three terms: the energy to stretch the C–C bond, the energy to form a new C–H bond, and the energy associated with the orbital distortions when the reactants come together:

$$V(\rho_{CC}, \rho_{CH}) = E_{CC}(\rho_{CC}) + E_{CH}(\rho_{CH}) + V_{Pauli} \tag{10.52}$$

where $V(\rho_{CC}, \rho_{CH})$ is the potential energy surface for the system, ρ_{CH} and ρ_{CC} are the lengths of the C–H and C–C bonds, E_{CC} is the energy to stretch the carbon–carbon bond as a function of the bond length, E_{CH} is the energy that one gains in forming a carbon–hydrogen bond, and V_{Pauli} is the energy associated with the orbital distortions.

Blowers and Masel approximated E_{CC} and E_{CH} by what are called *Morse potentials*:

$$E_{CC}(\rho_F) = w_{CC}([\exp(-\alpha_{CC}(\rho_{CC} - \rho_{CC}^e)) - 1]^2 - 1) \tag{10.53}$$

$$E_{CH}(\rho_{CH}) = w_{CH}([\exp(-\alpha_{CH}(\rho_{CH} - \rho_{CH}^e)) - 1]^2 - 1) \tag{10.54}$$

where ρ_{CC} and ρ_{CH} are the lengths of the C–C and C–H bonds; ρ_{CC}^e and ρ_{CH}^e are the equilibrium bond lengths; w_{CC} and w_{CH} are the bond dissociation energies for the carbon–carbon and carbon–hydrogen bonds in kcal/mol, which are available from the CRC (the CRC calls them *bond strengths*); and α_{CC} and α_{CH} are constants.

Figure 10.25 shows a plot of the Morse potential as a function of the bond length. The potential starts out high (i.e., very repulsive) and at short bond distances. The potential decreases as the bond length increases, reaching a minimum when $\rho_{CC} = \rho_{cc}^e$. The potential then goes to zero at long bond distances. If we change α_{CC}, the width of the minimum changes but the depth does not change. Real atomic potentials look very similar to this, which is why the Morse potential has proved so useful.

For the purposes of derivation, we will also assume that the Pauli repulsion can be approximated via a simple exponential:

$$V_{Pauli} = V_0 \exp(-\beta_{CC}\rho_{CC} - \beta_{CH}\rho_{CH}) \tag{10.55}$$

where β_{CC}, β_{CH}, and V_0 are constants.

Figure 10.26 shows a plot of a Pauli potential calculated from equation (10.55). The potential is small unless both the carbon–carbon and carbon–hydrogen bond lengths are small, which corresponds to the case where the reactants are close enough together that significant orbital distortions are seen. The potential stiffens as β increases.

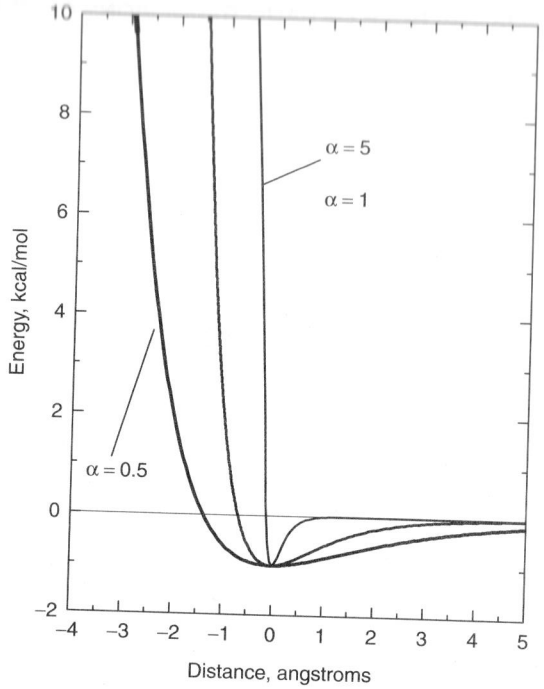

Figure 10.25 A Morse potential for different values of α_{CC}.

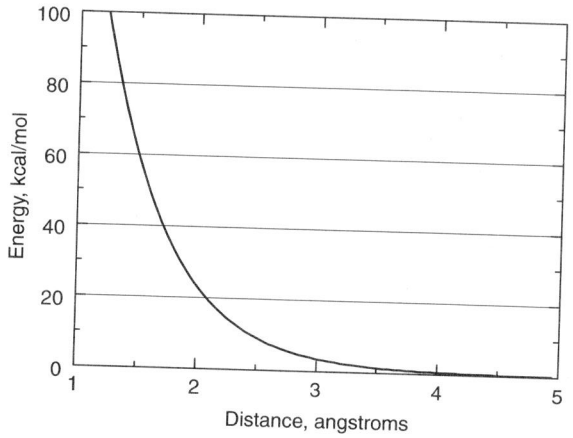

Figure 10.26 A plot of V_{Pauli} as a function of the interatomic distance for some typical values of the parameters.

Figure 10.27 compares some data for some helium–helium interactions to equation (10.55). Notice the good fit. Therefore, it seems that equation (10.55) is a good approximation.

Next we will derive an equation that allows us to calculate E_a from the Blowers–Masel model. Combining equations (10.52)–(10.55) yields what looks like a complex expression

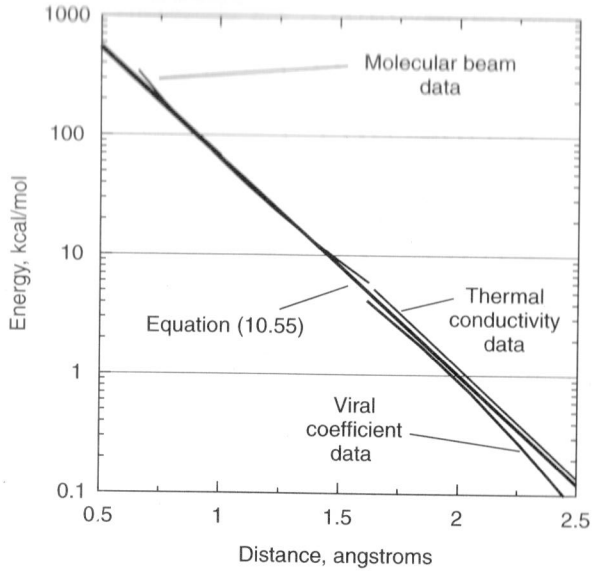

Figure 10.27 A comparison of Pauli repulsion determined experimentally for helium–helium collisions to that calculated from equation (10.55). [Data from Bernstein and Muckerman (1967)].

for the potential energy:

$$\begin{aligned} V(\rho_{CC}, \rho_{CH}) = {} & w_{CC}([\exp(-\alpha_{CC}(\rho_{CC} - \rho^e_{CC})) - 1]^2 - 1) - w_{CC} \\ & + w_{CH}([\exp(-\alpha_{CH}(\rho_{CH} - \rho^e_{CH})) - 1]^2 - 1) \\ & + V_0 \exp(-\beta_{CC}\rho_{CC} - \beta_{CH}\rho_{CH}) \end{aligned} \tag{10.56}$$

Figure 10.28 is a plot of the potential energy surface calculated from equation (10.59) for reaction (10.51). Blowers and Masel showed that the potential energy surface is virtually identical to the ab initio potential energy surface for the same reaction. Therefore, the model does reproduce the qualitative trends in the potential energy surfaces.

Next, we will simplify equation (10.56). First it is useful to define n_{CC} and n_{CH}, the Pauling bond order of the carbon–carbon and carbon–hydrogen bond, via

$$n_{CC} = \exp(-\alpha_{CC}(\rho_{CC} - \rho^e_{CC})) \tag{10.57}$$

$$n_{CH} = \exp(-\alpha_{CH}(\rho_{CH} - \rho^e_{CH})) \tag{10.58}$$

Pauling showed that with this definition, n_{CC} is 1.0 for a first-order bond and 2.0 for a second-order bond. During reaction (10.51), the $n_{CC} = 1.0$ and $n_{CH} = 0.0$ at the start of the reaction. As the reaction proceeds, n_{CC} decreases while n_{CH} increases, until at the end of the reaction $n_{CC} = 0.0$ while $n_{CH} = 1.0$.

Substituting equations (10.57) and (10.58) into equation (10.56) yields

$$\begin{aligned} V(n_{CC}, n_{CH}) = {} & w_{CC}([n_{CC} - 1]^2 - 1) - W_{CC} \\ & + w_{CH}([n_{CH} - 1]^2 - 1) + V_P(n_{CC})^{q_{CC}}(n_{CH})^{q_{CH}} \end{aligned} \tag{10.59}$$

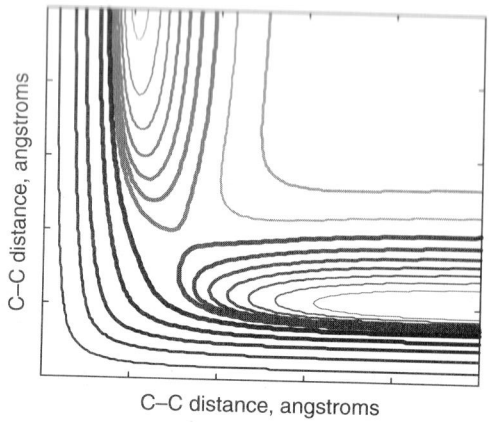

Figure 10.28 A potential energy surface calculated from equation (10.59) with $w_{CC} = 95$ kcal/mol, $w_{CH} = 104$ kcal/mol, $V_P = 300$ kcal/mol, $q_{CC} = 0.7$, $q_{CH} = 0.5$.

where

$$q_{CC} = \frac{\beta_{CC}}{\alpha_{CC}}, \qquad q_{CH} = \frac{\beta_{CH}}{\alpha_{CH}} \tag{10.60}$$

$$V_P = V_0 \exp(+\beta_{CC}\rho^e_{CC} + \beta_{CH}\rho^e_{CH}) \tag{10.61}$$

At the transition state

$$\frac{\partial V}{\partial n_{CC}} = 0, \qquad \frac{\partial V}{\partial n_{CH}} = 0 \tag{10.62}$$

Substituting equation (10.59) into equation (10.62), solving for n_{CC} and n_{CH}, and then substituting back into equation (10.59) allows one to derive an expression for the energy of the transition state. For special case that $q_{CC} = q_{CH} = 1$, Blowers and Masel find

$$E_a = \begin{cases} 0 & \text{when } \dfrac{\Delta H_r}{4E_a^0} < -1 \\ \dfrac{(w_0 + 0.5\Delta H_r)(V_P - 2w_0 + \Delta H_r)^2}{(V_P)^2 - 4(w_0)^2 + (\Delta H_r)^2} & \text{when } -1 \le \dfrac{\Delta H_r}{4E_a^0} \le 1 \\ \Delta H_r & \text{when } \dfrac{\Delta H_r}{4E_a^0} > 1 \end{cases} \tag{10.63}$$

where E_a is the activation barrier and

$$w_0 = \frac{w_{CC} + w_{CH}}{2} \tag{10.64}$$

It works out that V_P is related to the intrinsic barrier, E_a^0, by

$$V_P = 2w_0 \left(\frac{w_0 + E_a^0}{w_0 - E_a^0} \right) \tag{10.65}$$

In order to use equation (10.63), one first chooses E_a^0 and w_0, calculates V_P and then plugs into equation (10.65). The results are virtually independent of w_0. Consequently, one can use an average value of w_0 (i.e. 100 kcal/mol) in all of the calculations with little error.

10.7.1 Qualitative Features of the Model

The Blowers–Masel model makes four key predictions:

- The activation barrier varies nonlinearly with the heat of reaction, approaching zero for very exothermic reactions and ΔH_r for very endothermic reactions.
- There is no inverted region.
- The results are similar to the Marcus equation when $-1 \le \Delta H_r/4E_a^0 \le 1$.
- Increases in the bond energies can increase or decrease the intrinsic barriers to reaction.

Figure 10.29 compares the activation barriers computed from the Blowers–Masel model to the activation barrier to barriers computed from the Marcus equation. Both models give virtually identical results when -36 kcal/mol $\le \Delta H \le 36$ kcal/mol. However, there are derivations at higher energies. The barriers vary nonlinearly with the heat of reaction in qualitative agreement with Figure 10.11.

Still, the Marcus equation predicts and inverted region where E_a^0 grows to infinity for very exothermal reactions; no inverted behavior is seen with the Blowers–Masel model. The Blowers–Masel model also predicts that E_a approaches ΔH_r at large ΔH_r. While the Marcus equation predicts that E_a diverges from ΔH_r at large ΔH_r.

Figure 10.29 compares both models to data. Notice that the data seem to fit the Blowers–Masel model much better than does the Marcus equation. Physically, the

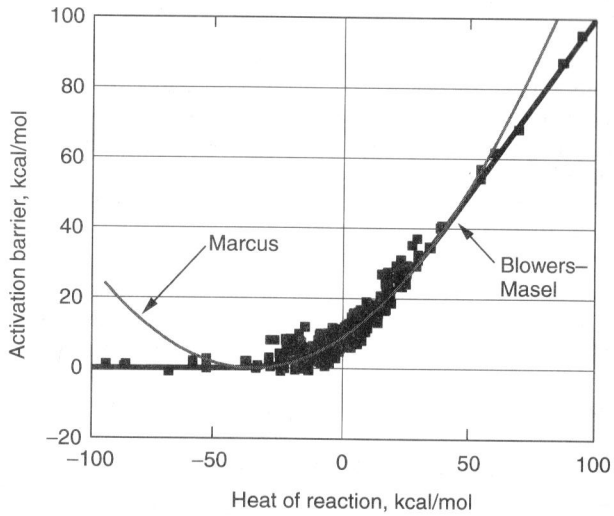

Figure 10.29 A comparison of the barriers computed from the Blowers–Masel model to barriers computed from the Marcus equation and to data for a series of reactions of the form $R + HR^1 \rightarrow RH + R^1$ with $w_0 = 100$ kcal/mol and $E_a^0 = 10$ kcal/mol.

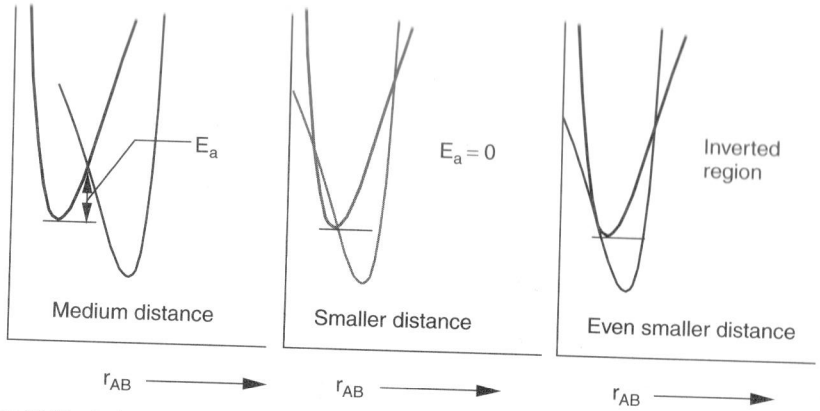

Figure 10.30 A plot of the changes in the curve crossing energy as two molecules come together during the reaction AB + C → A + BC.

Blowers–Masel model allows the size of the transition state to vary. Generally the reactants come together; specifically, $(r_2 - r_1)$ changes as the reaction occurs. One can imagine the potential energy surface as being constructed as a series of curve-crossing (see Figure 10.30) models. When the reactants are far away, there is a large barrier to reaction. However, as the distance decreases, the barrier decreases. You always get to the situation that the barrier is zero before you get into the inverted region. The reactants react when the barrier is zero, so the system never reaches the inverted region. As a result, the Blowers–Masel model does not allow Marcus inverted behavior to occur.

The other major difference between the Blowers–Masel model and the Marcus equation is that the Marcus equation predicts that increases in the bond energy in the reactants will always increase the intrinsic activation barrier. However, the Blowers–Masel model allows for nonmonotonic behavior. For example, Figure 10.31 shows the variation in the intrinsic barriers with changing bond strength, w_0, computed from the Blowers–Masel model with $V_P = 400$ kcal/mol. Notice that the intrinsic activation barrier increases and then decreases with increasing bond strength. Figure 10.31 also shows some ab initio results. The data show some similar trends, although the data do not fit equation (10.63) exactly. Physically, equation (10.63) does not fit exactly because of the assumption $q_{CC} = q_{CH} = 1$; if you adjust q_{CC} and q_{CH}, you can fit the data in Figure 10.31 exactly. The final equation $q_{CC} \neq 1$ is more complex than equation (10.63).

Physically, increases in the bond strength in the reactants make the bonds harder to break, which raises the intrinsic barrier to reaction. However, the increases in the bond strength also pull the reactants together. That decreases the size of the transition state, $(r_2 - r_1)$, which, in turn, lowers the intrinsic barrier to reaction. As a result, the intrinsic barriers to reaction can increase or decrease with increasing w_0, as shown in Figure 10.31.

One of the main advantages of the Blowers–Masel model is that it allows one to fit a wider data set than does the Marcus equation. For example, the data in Figure 10.17 are easily fit to the Blowers–Masel model, whereas they do not fit the Marcus equation. The Blowers–Masel model also allows one to fit data as shown in Figure 10.9. Thus, the model is useful.

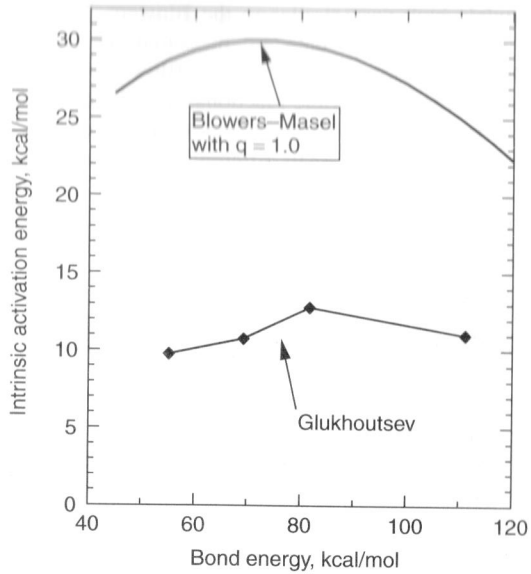

Figure 10.31 The variation in the intrinsic barrier with changing bond strength, w_0, computed from the Blowers–Masel model with $V_P = 400$ kcal/mol. Glukhoutsev's (1995) ab initio calculations of the activation barrier for the reaction $X + CH_3X \rightarrow XCH_3 + X$ are included for comparison.

10.7.2 Comparison of the models

Next, it is useful to compare the three models described so far in this chapter. Figure 10.32 shows a plot of the Marcus equation, the Polanyi relationship, and the Blowers–Masel approximation for identical sets of parameters. Notice that all three models are very similar. The data in Figure 10.29 follow the Blowers–Masel approximation most closely,

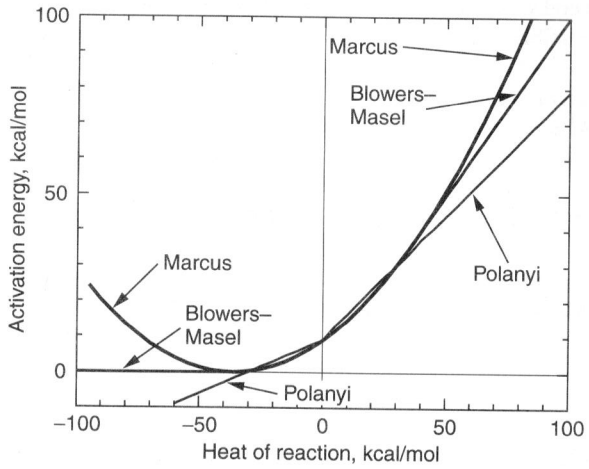

Figure 10.32 A comparison of the Marcus equation, the Polanyi relationship, and the Blowers–Masel approximation for $E_a^0 = 9$ kcal/mol and $w_0 = 120$ kcal/mol.

but the other two models look very similar to the Blowers–Masel approximation over the range of conditions where most data are measured (i.e., -50 kcal/mol $< \Delta H_r <$ 50 kcal/mol). The Marcus equation deviates from the Blowers–Masel approximation only for very endothermic and very exothermic reactions. In order to fit data with the Polanyi relationship, one needs to draw several lines. However, if one does that, one still fits data quite well. In practice, there are some small differences between the models; in particular, the Blowers–Masel model fits the data over the widest range. However, in practice, all three models give very similar predictions except for very endothermic or very exothermic reactions.

10.8 LIMITATIONS OF THE MODELS: QUANTUM EFFECTS

The big limitations of the models that we have discussed so far is that the models ignore quantum effects. One might initially suppose that quantum effects are not important to reactions. After all, bonds break, and most bonds look fairly classical. Still, there is one important class of reactions where the quantum effects are quite important: four-center reactions. Consider the following reaction:

$$H_2 + I_2 \longrightarrow 2HI \tag{10.66}$$

Years ago, people thought that reaction (10.66) proceeded by a four-centered reaction. Two bonds form during the reaction, and two are destroyed. Therefore, one could draw a stick diagram and show two bonds forming and two bonds breaking. However, if you work out the wavefunctions, it turns out that during the reaction, you end up either trying to put four electrons in a single molecular orbital, or having an electron with a spinup and a spindown simultaneously. Quantum-mechanically, one can put at most two electrons into an orbital, one with spinup and another with spindown. It is impossible for an electron to have two different spins at the same time. Therefore, it ends up that the bonding in the four-centered transition state is not possible.

In a more general way, reaction (10.66) cannot occur via a four-centered transition state because it is impossible to continuously transform the reactant wavefunctions into product wavefunctions. Instead, one must break some bonds before the reaction can proceed. This effect is not limited to four-centered reactions. There is a whole series of reactions called *symmetry-forbidden reactions* that have high barriers due to quantum effects.

10.9 THE CONFIGURATION MIXING MODEL

We are going to need to do a considerable amount of algebra before we can derive the key equations that we want to use to see whether the bonds are transformed smoothly during the course of a reaction. Pross (1985) summarized the key ideas from several groups in what he calls the **configuration mixing model**. The idea is to treat a reaction as a process where the reactant wavefunctions are continuously transformed into product wavefunctions.

The analysis builds on some of the concepts of MO theory, which we will describe in detail in Chapter 11. Recall that in MO theory, one can write the wavefunction, ψ, for any MO of a system as an antisymmetrized product of the wavefunctions, ϕ_a, of all of

the atoms in the system. For example, ψ_σ, the wavefunction for the σ bond in a diatomic molecule AB, is given by

$$\psi_\sigma = \frac{1}{\sqrt{2}}(\phi_A + \phi_B)(\overline{\phi_B} + \overline{\phi_A}) \tag{10.67}$$

where ϕ_A is the wavefunction for an electron in the bonding orbital of A with the spin pointing up, $\overline{\phi_A}$ is the wavefunction for an electron in the bonding orbital of A with the spin pointing down, ϕ_B is the wavefunction for an electron in the bonding orbital of B with the spin pointing up, $\overline{\phi_B}$ is the wavefunction for an electron in the bonding orbital of B with the spin pointing down, and ψ is the antisymmetrizer. There are three important MOs for excited states of this system: ψ^*_σ, the wavefunction for the σ^* orbital of the A–B molecule:

$$\psi_{\sigma^*} = \frac{1}{\sqrt{2}}(\phi_A - \phi_B)(\overline{\phi_A} - \overline{\phi_B}) \tag{10.68}$$

$\Psi_{A:^-B^+}$, the wavefunctions for both electrons on A:

$$\Psi_{A:^-B^+} = \phi_A\overline{\phi_A} \tag{10.69}$$

and $\Psi_{A^+B:^-}$, the wavefunctions for both electrons on B:

$$\Psi_{A^+B:^-} = \phi_B\overline{\phi_B} \tag{10.70}$$

According to the configuration interaction (CI) model described in Section 11.2, one can write the wavefunction for any state of the system as a sum of the Slater determinates for these MOs, plus the Slater determinates for additional excited states. For example, if A and B form a bond with a significant dipole moment, then the wavefunction for the bonding state of the system, $\Psi_{A–B}$, can be written as

$$\Psi_{A–B} = c_\sigma\psi_\sigma + c_{A:^-B^+}\Psi_{A:^-B^+} + c_{A^+B:^-}\Psi_{A^+B:^-} + c_{\sigma^*}\psi_{\sigma^*} \tag{10.71}$$

where we used Ψ rather than ψ in equation (10.71) to indicate that $\Psi_{A–B}$ is a wavefunction that has been computed with the CI model. Similarly, $\Psi_{A\bullet B\bullet}$, the wavefunction for one electron being on A and one being on B with no interaction between the two, is

$$\Psi_{A\bullet B\bullet} = \frac{1}{\sqrt{2}}(\psi_\sigma + \psi^*_\sigma) \tag{10.72}$$

For the discussion that follows, we will designate the wavefunction in equation (10.72) as the [A•B•] state of the system, and the wavefunction in equation (10.71) as the [A–B] state of the system. In some cases, it will also be useful to discuss the [A^+B^-] state of the system. The [A^+B^-] state of the system is just the [A–B] state in the limit $|c_{A^+B:^-}| \gg |c_\sigma|$, $|c_{A:^-B^+}|$, $|c_{\sigma^*}|$.

In the material that follows, we will consider how the electronic configuration of the A–B molecule changes as a reaction proceeds and use that information to predict the activation barrier for the reaction between A and B.

The derivation will start with a simple example where a sodium atom approaches a chlorine atom and reacts to form sodium chloride:

$$Na\bullet + Cl\bullet \longrightarrow Na^+Cl^- \tag{10.73}$$

When the two atoms are far apart, the [Na•Cl•] configuration is the ground state of the system while $[Na^+Cl^-]$ configuration is the first excited state. In contrast, in sodium chloride, $[Na^+Cl^-]$ state is the ground state and the [Na•Cl•] state is the first excited state.

Now consider doing a thought experiment where a sodium atom approaches a chlorine atom but the sodium atoms and the chlorine atom are prevented from exchanging electrons. According to calculations, when the sodium atom approaches the chlorine atom, the energy of both the [Na•Cl•] and $[Na^+Cl^-]$ configurations go down as indicated in Figure 10.33. However, the $[Na^+Cl^-]$ configuration is stabilized much more than is the [Na•Cl•] configuration. That is why the equilibrium structure is $[Na^+Cl^-]$.

Now, let's do the same process but allow the sodium atom and chlorine atom to exchange electrons. When the sodium atom and the chlorine atom initially approach one another, they start out in the [Na•Cl•] configuration. However, during the reaction, there is an exchange of electrons between the sodium and the chlorine to yield the $[Na^+Cl^-]$ species. The exchange of electrons occurs gradually during the course of the reaction. At any point along the reaction coordinate, one can represent the electronic structure of the system as a mixture of the [Na•Cl•] and $[Na^+Cl^-]$ configurations.

For future reference, we will indicate the reaction pathway as the lower dashed line in Figure 10.33. The reactants start out in the [Na•Cl•] configuration, but, as the reaction

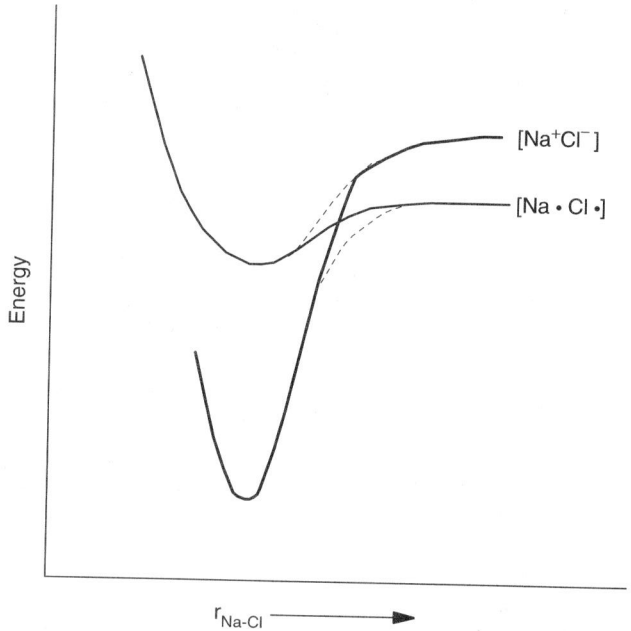

Figure 10.33 A schematic showing how the energy of the [Na•Cl•] and $[Na^+Cl^-]$ configurations of NaCl change as a sodium atom approaches a chlorine atom.

proceeds, there is a continuous change in the configuration of the system from the [Na•Cl•] state into the $[Na^+Cl^-]$ state.

Note that if you did not get mixing of the configurations, the sodium and the chlorine would stay in the [Na•Cl•] configuration. The atoms could not get into the $[Na^+Cl^-]$ configuration. Hence, one would not get any reaction. As a result, it is the mixing of configurations that allows the sodium and chlorine reaction to form (metastable) sodium chloride.[1]

This example illustrates the idea that reactions can be represented as a conversion of the electronic structure of the reactants from one configuration to another. In the following discussion, we will model the changes in electronic structures, and use that information to make prediction about reactions.

We will start by noting that the conversion of one state into another can be modeled as something called an **avoided crossing**. Notice that if there were no interactions between the [Na•Cl•] and $[Na^+Cl^-]$ configurations of sodium chloride, the curves for the energies of the two states in Figure 10.33 would cross. In reality, however, there are strong interactions between the two configurations. In Section 10.9.1, we will show that when two states interact, they mix to form an upper state whose energy is greater than that of either of the two individual states, and a lower state whose energy is lower than that of either of the two individual states. The energy of the two states are represented by the dashed line in Figure 10.33. Notice that because of the interactions between the [Na•Cl•] and $[Na^+Cl^-]$ configurations, the energies of the eigenstates of the system never cross; hence the name **avoided crossing**. One does not always get avoided crossings when energy curves for reactions cross. Later in this chapter, we will provide several examples where the curves actually cross. However, the significance of the avoided crossing is that it provides a mechanism to allow the system to change from one configuration to another. When avoided crossings happen, one can continuously transfer an electron from one state of the system to another. That allows bonds to rearrange so that a reaction can take place. If there is no avoided crossing, there is no change in the configuration of the reactants and hence no reaction. As a result, avoided crossings are very important to the theory of reactions.

Woodward and Hoffmann (1970) show that one can model most reactions as a change in the electronic configuration of the reactants and an avoided crossing. (The main exception is in photochemical reactions where the change in configuration can be driven by a photon rather than an avoided crossing.) Hence, the idea of describing a reaction as a change in the electronic configuration of the reactants with an avoided crossing is quite useful.

In the materials to follow, it will be useful to draw what is called a *configuration mixing diagram for a reaction*, where the configuration mixing diagram is a plot showing the energy of each of the configurations of the system change as a function of the reaction coordinate (e.g., bond order). The diagram also shows how the states mix.

Figure 10.34 shows a configuration mixing diagram for the reaction of a sodium atom with a chlorine atom. The configuration mixing diagram for the reaction between a sodium atom and a chlorine atom contains the same information as was given in Figure 10.33. There are two solid lines in the coordination mixing diagram: one starting at the [Na•Cl•] state of the reactants and going to the [Na•Cl•] state in the products, and the other starting at the $[Na^+Cl^-]$ state in the reactants and going to the $[Na^+Cl^-]$ state in the products. There are also dashed lines indicating the avoided crossing. The implication

[1] As noted in Chapter 8, when an isolated sodium atom reacts with an isolated chlorine atom, a considerable amount of energy is released. The energy needs to be dissipated before a stable NaCl crystal can form. As a result, initially reaction (10.73) produces a hot metastable complex not crystalline sodium chloride.

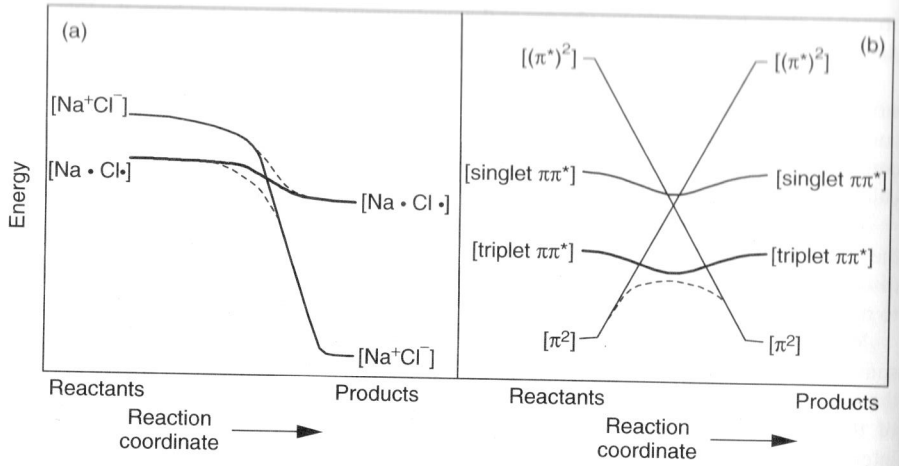

Figure 10.34 Configuration mixing diagram for (a) Na• + Cl• → NaCl, (b) conversion of *cis*-butene to *trans*-2-butene.

of this configuration mixing diagram is that during the reaction, the [Na•Cl•] and the [Na^+Cl^-] states mix continuously to convert the reactants to products.

Figure 10.34 also shows the configuration mixing diagram for the conversion of *cis*-butene, into *trans*-butene.

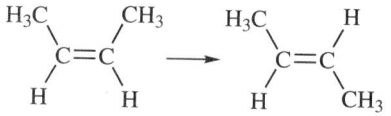

(10.74)

The system starts outs with two p electrons in a π^2 orbital. For future reference, we note that there are several excited states of the system: a triplet $\pi\pi^*$ state, a singlet $\pi\pi^*$ state, and a singlet $(\pi^*)^2$ state. Now consider what happens when one rotates the $:CHCH_3$ group in the right half of *cis*-2-butene around the carbon–carbon bond, leaving the $CH_3HC:$ group on the left fixed. Note that the rotation reverses the sign of all of the p orbitals on the right $:CHCH_3$ group. We start out with an electron in a π orbital with a wavefunction, ψ_π, given by

$$\psi_\pi = \frac{1}{\sqrt{2}}(\phi_{p\cdots left} + \phi_{p\cdots right}) \tag{10.75}$$

where $\phi_{p\cdots left}$ and $\phi_{p\cdots right}$ are the wavefunctions for the p orbitals on the left and right $:CHCH_3$ group. Notice that when we rotate the right $:CH_2CH_3$ group $\phi_{p\cdots right}$ is converted into $-\phi_{p\cdots right}$. As a result, the π orbital is converted into a π^* orbital with

$$\psi_\pi = \frac{1}{\sqrt{2}}(\phi_{p\cdots left} - \phi_{p\cdots right}) \tag{10.76}$$

Similarly, the π^* orbitals are converted to bonding π orbitals. As a result, the original $(\pi^*)^2$ state is converted into the ground state of the system while the original π^2 state is converted into a $(\pi^*)^2$ state.

Now consider what happens as the reaction proceeds. We start within the π^2 state. However, as we begin to twist the molecule, we begin to mix in some of the excited states. First, the triplet $\pi\pi^*$ state begins to interact with the π^2 state. Later the original $(\pi^*)^2$ state plays a role. This diagram illustrates two important conclusions from the configuration mixing model: (1) the mixing of excited states with the ground state plays an important role in determining the potential energy surface for a reaction, and (2) often many different excited states play a role in the reaction.

The idea that the mixing of the ground state with the excited states of the system determines potential energy surfaces provides an alternative view of why reactions are activated.

Recall that when people first started to apply reaction rate theory, it was not obvious why activation barriers arose during reactions. The reaction of hydrogen atoms with a deuterium tritium molecules illustrates the difficulty:

$$H + DT \longrightarrow HD + T \tag{10.77}$$

Note that as this reaction proceeds, a deuterium–tritium bond breaks and a hydrogen–deuterium bond forms. Initially, there is a single D–T bond. Half way through the reaction, there is half a H–D bond and half a D–T bond. At the end of the reaction, there is a single H–D bond. Hence, the total bond order is conserved during reaction.

Up to the 1990s, people thought that reactions were activated because bonds broke during reaction. We now know that the barrier for reaction (10.77) occurs because orbitals are distorted. In fact, when one does a quantum calculation of the barriers, one writes the wavefunction for the system ψ as a sum of the wavefunctions for all of the states in the system ϕ_m:

$$\psi = \sum_{states,m} C_m\phi_m \tag{10.78}$$

In equation (10.78) the C_m terms are a series of coefficients and ϕ_m is the wavefunction for the mth state of the system. When orbitals distort, one finds that one gets contributions to ψ from the excited states of the system. As a result, one can say that one is mixing excited states into the ground state as the reaction proceeds.

The configuration mixing model explains in part why activation barriers arise during reaction. The general idea is that as a reaction proceeds, excited states are mixed into the ground-state wavefunction. The mixing of excited states raises the energy of the system and hence produces an activation barrier. Physically, when excited states get mixed into the ground-state wavefunction, the wavefunctions are distorted. Hence, one might want to think about a barrier as being associated with distortion of orbitals in the reactants as a reaction proceeds.

It is useful to consider how the Marcus–Polanyi relationship arises from the configuration mixing model. In the next few pages, we will show that the Marcus equation arises naturally from the configuration mixing model. Our approach will be to start with a two-state model where one of the states represents the reactant configuration while the other state represents the product configuration. We will then consider how a substituent affects the energy of each states. An analysis similar to that in Section 11.5 will be used to derive an equation analogous to the Marcus equation.

Consider the following reaction:

$$A\bullet + B\bullet \longrightarrow A^+ + B^- \tag{10.79}$$

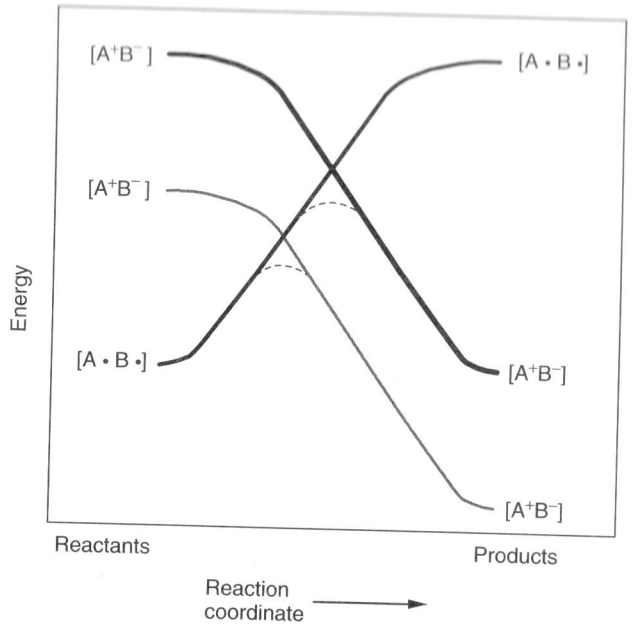

Figure 10.35 Configuration mixing model for the reaction $A\bullet + B\bullet \rightarrow A^+ + B^-$ showing how changes in the energy of the [AB] configuration affect the reaction.

A configuration mixing diagram for the reaction is shown as the solid line in Figure 10.35. The [A•B•] configuration is the ground state of the reactants and an excited state of the products, while the $[A^+B^-]$ configuration is an excited state of the reactants and the ground state of the products. During the reaction, the configuration of the system moves up the [A•B•] curve and then down the $[A^+B^-]$ curve.

Now consider making a change that displaces the curve for the $[A^+B^-]$ state up or down. Notice that such a displacement will cause the activation barrier to change. One can model the change by examining how the interaction between the curves shift up or down as the reaction proceeds.

Notice the close correspondence between the configuration mixing diagram in Figure 10.35 and the Polanyi diagram in Figure 10.13. In both cases, the activation barrier is given as a curve crossing on a reaction coordinate diagram. Hence, the analysis in Section 11.5 also applies to the configuration mixing diagram Figure 10.35. In particular, if we fit the curves in Figure 10.35 to lines, we can derive the Polanyi relationship. If we fit the curves to parabolas, we will derive the Marcus equation. Hence, the Polanyi relationship and Marcus equation apply as well to the situation depicted in Figure 10.35 as to the situation described in Section 10.5.

Pross and Shalk showed that one could use the configuration mixing model to calculate the intrinsic barrier for reaction. The idea is that in the configuration mixing model, intrinsic barriers are associated with the energy to move electrons from one MO to another. If one models the interaction between the system as a curve crossing, then one can get some information about the barriers from Figure 10.36.

Figure 10.36 shows four cases. The first two cases show how changes in the gap between the reactions affects the barriers to reaction. Notice that as you increase the gap,

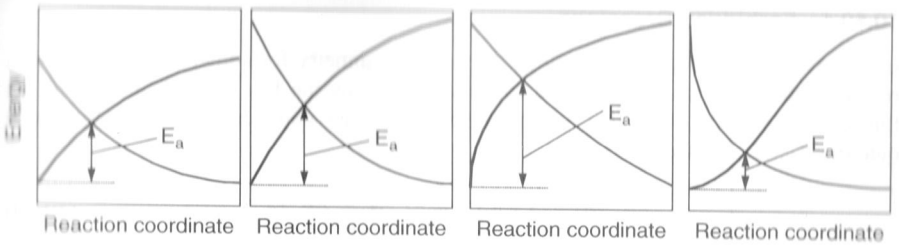

Figure 10.36 A diagram showing how changes in the configuration mixing model affects the intrinsic barrier to reaction.

it costs more energy to put an electron into an excited state. Consequently, it costs more energy to mix in the excited state. That raises the barriers to reaction.

Another way to change the barriers is to change the slopes in Figure 10.36. Notice that as the slopes decrease, the barriers decrease. Physically, the slopes are a measure of how much of the excited state is mixed into the ground state during the initial stages of reaction. If the orbitals in the reactions are distorted more, the initial contribution from the excited states will grow. That will raise the barriers to reaction. Generally, the configuration mixing model makes predictions that are similar to those of the Blowers–Masel model. Further, the configuration mixing model allows you to quantify the barriers to reaction; the details will be discussed in Chapter 11.

Unfortunately, the configuration mixing model does not work in detail. The key assumption in the configuration mixing model is that one can write the wavefunction for the transition state as a sum of terms such as that in equation 10.71, where all the terms in the sum are wavefunctions for states of the reactants. Quantum-mechanically, that is not correct. Physically, when a reaction occurs, bonds are extended. The extended bonds contain contributions from orbitals that are bigger than the orbitals in the reactants. In particular, big orbitals called "diffuse functions" play a key role. The big orbitals are missing from the sum in equation (10.71). As a result, the configuration mixing model does not work in detail.

10.10 SYMMETRY-FORBIDDEN REACTIONS

Another source of derivations from the configuration mixing model occurs during something called a **symmetry-forbidden reaction**. Throughout the last section, we assumed that when the energy contours for two states of the system cross, the states will mix to provide a pathway for a reaction. However, in 1965, Woodward and Hoffmann (1965a,b,c) noted that sometimes states cannot mix. When states do not mix, one does not have a convenient pathway to convert the reactants into products. As a result, the reaction rate is negligible. Hoffmann showed that the states will not mix when the symmetries of the states are wrong. Hence, he called reactions that show negligible rates, because the reactant and product configurations do not mix, **symmetry-forbidden reactions**.

Woodward and Hoffmann (1970) wrote a famous book, *The Conservation of Orbital Symmetry*, which describes, in detail, the role of symmetry in determining rates of reactions. In the materials that follow, we will summarize the key ideas from Woodward and Hoffmann's analysis. We will also review some other interpretations of the ideas due to Pearson (1976) and Fukui (1975). One should refer to Woodward/Hoffmann (1970), Pearson (1976), or Fukui (1952,1957,1975) for further details.

10.10.1 Forbidden Crossings

In the next several sections, we will be discussing symmetry-forbidden reactions, namely, reactions that cannot occur because symmetry prevents the key states from mixing. In this section, we will show that one can determine when states can mix by examining a quantity $\beta_{10}(\mathcal{X})$ defined by

$$\beta_{10}(\mathcal{X}) = \iiint \Psi_1^*(\mathcal{X})\mathcal{H}_1(\mathcal{X})\Psi_0(\mathcal{X})\,d\vec{r} \tag{10.80}$$

where $\Psi_0(\mathcal{X})$ is the wavefunction for the initial state of the system, $\Psi_1^*(\mathcal{X})$ is the wavefunction for the final state of the system, and $\mathcal{H}$ is called the *transition Hamiltonian*. States can mix whenever β_{10} is nonzero. No mixing occurs when β_{10} is zero. The derivation is complex and could be skipped without difficulty. It is useful to consider when states can mix. Consider a reaction where molecules A and B come together and react. When the two molecules are far apart, we can describe the electronic structure of the system by a Hamiltonian, $\mathcal{H}_0^0$, with a ground-state wavefunction Ψ_0, and a first excited-state wavefunction Ψ_1^0, where Ψ_0^0 and Ψ_1^0 satisfy

$$\mathcal{H}_0^0\Psi_0^0 = E_0^0\Psi_0^0 \tag{10.81}$$

$$H_0^0\Psi_1^0 = E_1^0\Psi_1^0 \tag{10.82}$$

with $E_0^0 < E_1^0$.

Now consider doing a thought experiment where we move the two molecules together but do something to prevent the two molecules from reacting. Let's define a Hamiltonian for the nonreactive case as $\mathcal{H}_0(\mathcal{X})$, where we have noted that $\mathcal{H}_0$ is a function of $\mathcal{X}$, where $\mathcal{X}$ is a generalized reaction coordinate. We will assume that when $\mathcal{X} = 0$, $\mathcal{H}_0(\mathcal{X})$ will equal the reactant Hamiltonian and when $\mathcal{X} = 1$, $\mathcal{H}_0(\mathcal{X})$ will equal the product Hamiltonian. We will also define $\Psi_0(\mathcal{X})$ and $\Psi_1(\mathcal{X})$ to be the eigenstates of the Hamiltonian that need to mix for the reaction to occur, and we will define $E_0(\mathcal{X})$ and $E_1(\mathcal{X})$ to be the corresponding eigenvalues of $\mathcal{H}_0(\mathcal{X})$.

Figure 10.37 shows a configuration mixing diagram for the reaction between A and B. The solid lines in the figure are plots of $E_0(\mathcal{X})$ and $E_1(\mathcal{X})$ as a function of the reaction coordinate. We have set up the system so that during the reaction Ψ_0 changes from the ground state to the first excited state while Ψ_1 changes from the first excited state to the ground state.

Now consider moving the molecules together and trying to get the reaction to occur. When reaction occurs, the Hamiltonian of the system will be different from $\mathcal{H}_0$, so let's call the new Hamiltonian $\mathcal{H}_1(\mathcal{X})$. For the derivation that follows, it is useful to define a constant $(\mathcal{H})$ by

$$\mathcal{H}_1(\mathcal{X}) = \mathcal{H}_0(\mathcal{X}) + \mathcal{H}(\mathcal{X}) \tag{10.83}$$

The question that we want to address is whether the two states can mix when the atoms move together, so let's assume that the new ground state of the system has a wavefunction $\Psi'(\mathcal{X})$ that is a mixture of the wavefunctions for the two original configurations:

$$\Psi'(\mathcal{X}) = C_0(\mathcal{X})\Psi_0(\mathcal{X}) + C_1(\mathcal{X})\Psi_1(\mathcal{X}) \tag{10.84}$$

We want the new wavefunction to satisfy

$$\mathcal{H}_1(\mathcal{X})\Psi'(\mathcal{X}) = E'(\mathcal{X})\Psi'(\mathcal{X}) \tag{10.85}$$

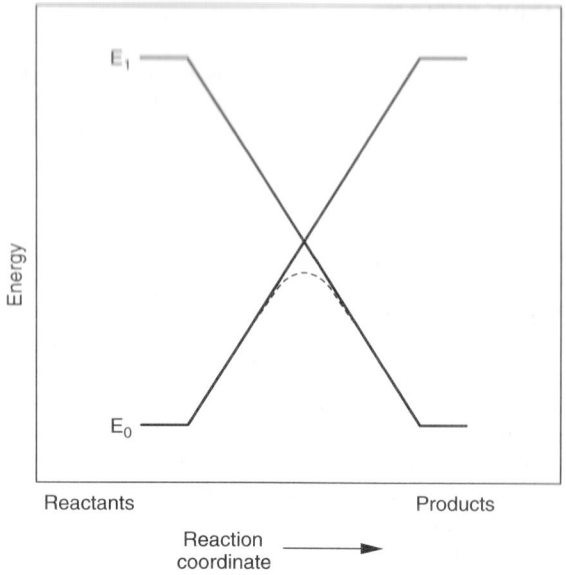

Figure 10.37 A configuration mixing diagram for a hypothetical reaction between A and B.

A detailed derivation is given in Masel (1996). Masel shows that there are two energy levels of the system with energies given by

$$E'_-(\mathcal{X}) = \frac{E'_0(\mathcal{X}) + E'_1(\mathcal{X})}{2} - \frac{\sqrt{(E'_0(\mathcal{X}) - E'_1(\mathcal{X}))^2 + 4\beta_{01}(\mathcal{X})\beta_{10}(\mathcal{X})}}{2} \tag{10.86}$$

$$E'_+(\mathcal{X}) = \frac{E'_0(\mathcal{X}) + E'_1(\mathcal{X})}{2} + \frac{\sqrt{(E'_0(\mathcal{X}) - E'_1(\mathcal{X}))^2 + 4\beta_{01}(\mathcal{X})\beta_{10}(\mathcal{X})}}{2} \tag{10.87}$$

and wavefunctions given by

$$\Psi_-(\mathcal{X}) = \begin{cases} \Psi_a(\mathcal{X}) & \text{when} \quad E_0(\mathcal{X}) \le E_1(\mathcal{X}) \\ \Psi_b(\mathcal{X}) & \text{otherwise} \end{cases} \tag{10.88}$$

$$\Psi_+(\mathcal{X}) = \begin{cases} \Psi_a(\mathcal{X}) & \text{when} \quad E_0(\mathcal{X}) \le E_1(\mathcal{X}) \\ \Psi_b(\mathcal{X}) & \text{otherwise} \end{cases} \tag{10.89}$$

with

$$\Psi_a(\mathcal{X}) = \frac{\Psi_0(\mathcal{X}) + \left(\dfrac{\beta_{10}(\mathcal{X})}{E'_-(\mathcal{X}) - E'_1(\mathcal{X})}\right)\Psi_1(\mathcal{X})}{\sqrt{1 + \left(\dfrac{\beta_{10}(\mathcal{X})}{E'_-(\mathcal{X}) - E'_1(\mathcal{X})}\right)^2}} \tag{10.90}$$

$$\Psi_b(\mathcal{X}) = \frac{\Psi_1(\mathcal{X}) + \left(\dfrac{\beta_{01}(\mathcal{X})}{E'_+(\mathcal{X}) - E'_0(\mathcal{X})}\right)\Psi_0(\mathcal{X})}{\sqrt{1 + \left(\dfrac{\beta_{01}(\mathcal{X})}{E'_+(\mathcal{X}) - E'_0(\mathcal{X})}\right)^2}} \tag{10.91}$$

10.11 QUALITATIVE RESULTS

Now, let's consider what happens when a reaction occurs. At the start of the reaction $\beta_{10}(\mathcal{X}) = 0$, so $\Psi_-(\mathcal{X}) = \Psi_0(\mathcal{X})$. Now, let's assume that when the molecules come together, $\beta_{10}(\mathcal{X})$ is nonzero. Note that according to equation (10.90), when $\beta_{10}(\mathcal{X})$ is nonzero, we get mixing of the states. If $\beta_{10}(\mathcal{X})$ is nonzero, the final wavefunction will approach $\Psi_1(\mathcal{X})$. Therefore, a reaction can occur whenever $\beta_{10}(\mathcal{X})$ is nonzero when the molecules collide.

The dashed line in Figure 10.37 is a plot of E as a function of $\mathcal{X}$ for a typical value of $\beta_{10}(\mathcal{X})$. Note that when $\beta_{10}(\mathcal{X})$ is nonzero, the energy of the lower eigenstate goes up over a hill and eventually ends up at E_0. This is typical for a reaction.

10.11.1 Reactions with Negligible Coupling

Note, however, that there are some cases where $\beta_{10}(\mathcal{X})$ is zero when two molecules collide. When $\beta_{10}(\mathcal{X})$ is zero throughout the collision process, $\Psi_-(\mathcal{X})$ is equal to Ψ_0 as the reactants come together. Hence, there would be no coupling of the state. Therefore, we conclude that the motion of the nuclei will convert one configuration of a system into another only when $\beta_{10}(\mathcal{X})$ is nonzero during the collision.

For future reference, we will call $\beta_{10}(\mathcal{X})$ the **coupling constant**, and note that reactions occur only when the coupling constant is nonzero.

In Nobel Prize–winning work, Woodward and Hoffmann (1970) provided several examples where $\beta_{10}(\mathcal{X})$ was zero during a reaction. In this section, we will consider a simple example that shows how $\beta_{10}(\mathcal{X})$ can be zero. One should refer to Woodward and Hoffmann (1970) or Pearson (1976) for many other examples.

Consider the following simple reaction:

$$H_2 + D_2 \longrightarrow 2HD \tag{10.92}$$

One can imagine that the reaction can go by either the chain propagation mechanism shown in Figure 10.38 or the four-centered reaction shown in Figure 10.39. Wright (1970, 1975) has also proposed a concerted six-centered reaction (e.g., $2H_2 + D_2 \rightarrow H_2 + 2HD$).

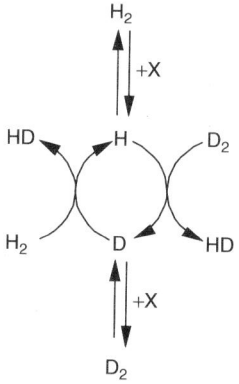

Figure 10.38 The chain propagation mechanism for H_2/D exchange.

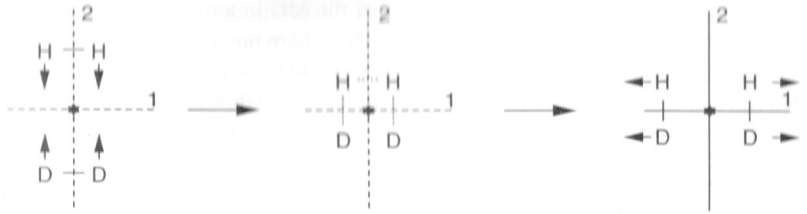

Figure 10.39 A hypothetical four-centered mechanism for H_2/D_2 exchange. The dotted lines in the figure denote mirror planes that are preserved during the reaction (see the text). This reaction is symmetry-forbidden.

At first sight one might think that the four-centered reaction would dominate. The six-centered reaction requires three molecules to come together simultaneously in the gas phase which is highly improbable. The first step in the chain propagation mechanism (Figure 10.38) is hydrogen–hydrogen bond scission. Hydrogen–hydrogen bond scission is highly activated. In contrast, superficially, during the four-centered reaction one is simply exchanging bonds within the molecule. As we have drawn the picture, there is no change in bond order anywhere in the reaction. Hence, from a superficial analysis, one might conclude that the four-centered reaction is possible.

In fact, however, the four-centered reaction has never been observed. At high temperatures, reaction (10.92) goes via the chain propagation mechanism. There has been some discussion about the mechanism at low temperatures where the six-centered reaction may predominate. However, there is no evidence that the reaction ever occurs at a measurable rate via a four-centered reaction. Calculations of Conroy and Malli (1969) indicate that the four-centered reaction has an activation energy of 515 kJ/mol! By comparison, the H–H bond strength is only 435 kJ/mol.

In the next few paragraphs, we will show that the reason why the reaction does not occur via the four-centered reactions is that the β_{10} values for the transformation of some of the reactant configurations in reaction (10.92) into production configurations are zero. As a result, the reaction in Figure 10.39 cannot occur via a simple gas-phase collision.

In order to derive the key results, it will be useful to view the reaction by sitting on a point half way between the hydrogen and the deuterium as indicated by the dot in Figures 10.39 and 10.40. One can imagine a transition state where there are both H–H and H–D bonds. If we model this transition state as one big molecule, then we can use molecular orbital (MO) theory to tell us how the configuration of the molecule changes as the reaction proceeds. There are four key MOs in the system. They are depicted in

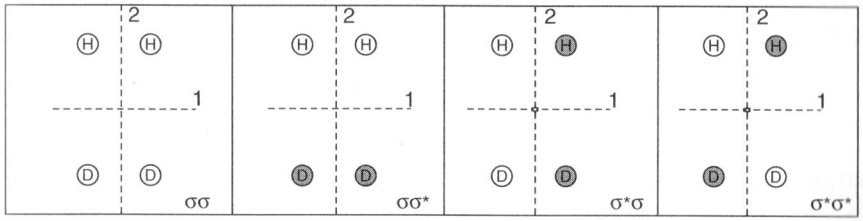

Figure 10.40 A schematic of the key molecular orbitals for the transition state of reaction (10.92). Positive atomic orbitals are depicted as open circles; negative orbitals are depicted as shaded circles.

Figure 10.40. For further reference, we will label the MO in terms of the bonding of one of the hydrogen atoms. The $\sigma\sigma$ MO will be an MO where one of the hydrogens is bound to the other hydrogen via a sigma bond between the hydrogens, and a σ^* bond between the hydrogens and the deuteriums. Figure 10.40 shows a schematic of the wavefunctions for the various states. All of the orbitals in the wavefunction for the $\sigma\sigma$ state, $\psi_{\sigma\sigma}$, have the same sign. In $\psi_{\sigma\sigma^*}$, the orbitals on both hydrogens have the same sign, but the orbitals on the two deuteriums have opposite signs. In $\psi_{\sigma^*\sigma}$, the orbitals on each adjacent H–D have the same sign but the orbitals on the H–H and D–D have opposite signs. In $\psi_{\sigma^*\sigma^*}$, the wavefunction for the orbitals has alternating signs.

Now consider what happens when we move the H_2 and D_2 together. We start out with no net interaction between the H_2 and D_2, so the wavefunction for the system $\Psi_{\text{reactants}}$ can be approximated by

$$\Psi_{\text{reactants}} = \psi_{\sigma\sigma}\psi_{\sigma\sigma^*} \tag{10.93}$$

At the end of the reaction, there are H–D bonds, but there are no net interactions between the two HD. Therefore, the wavefunction for the products Ψ_{products} can be approximated by $\psi_{\text{products}} = \psi_{\sigma\sigma}\psi_{\sigma^*\sigma}$. As a result, during the reaction electrons are moved from the $\sigma\sigma^*$ to the $\sigma\sigma^*$ MO.

Woodward and Hoffmann (1970) show that it is convenient to represent the transfer of electrons by a correlation diagram where the correlation diagram is very similar to a configuration mixing diagram. We keep track of what happens to each individual MO (i.e., the ψs) while in the configuration mixing diagram, and we keep track of what happens to the total wavefunction for the system (i.e., the Ψs).

Figure 10.41 shows a correction diagram for the four-centered reaction depicted in Figure 10.39. The reaction starts out with $\sigma\sigma$ and $\sigma\sigma^*$ MOs occupied and the $\sigma^*\sigma$ and $\sigma^*\sigma$ MOs empty. However, during the reaction, electrons are moved from the $\sigma\sigma^*$ to the $\sigma^*\sigma$ MO.

Now the questions is, whether the reaction can occur as depicted in Figure 10.39. According to the results in Section 10.11, the motion of the H_2 and D_2 toward one

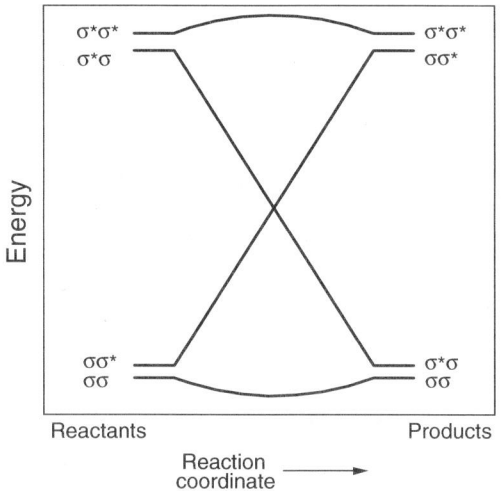

Figure 10.41 A correlation diagram for the reaction depicted in Figure 10.39.

another in the configuration shown in Figure 10.39 will allow the electrons in the $\sigma\sigma^*$ MO to be moved into the $\sigma^*\sigma$ MO whenever β is nonzero. Therefore, we can tell if reaction can occur by computing β. For further discussion, we will note that there are two mirror planes in Figure 10.39: one that lies half way between the H and the D_2, and, one that goes between the midpoints of the H–H and D–D bonds. We will designate those two mirror planes as planes 1 and 2.

According to equation (10.80), the coupling constant for conversion of the $\sigma\sigma^*$ state into the $\sigma^*\sigma$ state $\beta_{(\sigma\sigma^*)(\sigma^*\sigma)}$ is given by

$$\beta_{(\sigma\sigma^*)(\sigma^*\sigma)} = \iiint \psi^*_{\sigma\sigma^*}\mathcal{H}\psi_{\sigma^*\sigma}\,d\vec{\tau} \tag{10.94}$$

Note that $\mathcal{H}$ is completely symmetric. Assume that the interaction of the two mirror planes is the origin for Figure 10.39. If we move up, we move in the y direction. If we move to the right, we move in the positive x direction. Note that from symmetry

$$\mathcal{H}(x, y) = \mathcal{H}(-x, y) = \mathcal{H}(x, -y) = \mathcal{H}(-x, -y) \tag{10.95}$$

It is useful to rewrite equation (10.94) as

$$\begin{aligned}\beta_{(\sigma\sigma^*)(\sigma^*\sigma)} = &\int_0^\infty\int_0^\infty \psi_{\sigma\sigma^*}\mathcal{H}\psi_{\sigma^*\sigma}\,dx\,dy + \int_0^\infty\int_{-\infty}^0 \psi^*_{\sigma\sigma^*}\mathcal{H}\psi_{\sigma^*\sigma}\,dx\,dy \\ &+ \int_0^\infty\int_{-\infty}^0 \psi^*_{\sigma\sigma^*}\mathcal{H}\psi_{\sigma^*\sigma}\,dx\,dy + \int_{-\infty}^0\int_{-\infty}^0 \psi^*_{\sigma\sigma^*}\mathcal{H}\psi_{\sigma^*\sigma}\,dx\,dy\end{aligned} \tag{10.96}$$

For the purposes of derivation, it is useful to define a quantity "INT" by

$$\text{INT} = \int_0^\infty\int_0^\infty \psi_{\sigma\sigma^*}\mathcal{H}\psi_{\sigma^*\sigma}\,dx\,dy \tag{10.97}$$

Now consider a quantity INT′ given by

$$\text{INT}' = \int_0^\infty\int_{-\infty}^0 \psi^*_{\sigma\sigma^*}\mathcal{H}\psi_{\sigma^*\sigma}\,dx\,dy \tag{10.98}$$

INT is related to INT′ by a transformation that switches y with −y. Notice that when we switch y to −y, $\psi_{\sigma^*\sigma}$ does not change while $\psi_{\sigma\sigma^*}$ is converted into $-\psi_{\sigma\sigma^*}$. Therefore

$$\text{INT}' = -\text{INT} \tag{10.99}$$

A similar argument shows

$$\int_0^\infty\int_{-\infty}^0 \psi^*_{\sigma\sigma^*}\psi_{\sigma^*\sigma}\,dx\,dy = -\text{INT} \tag{10.100}$$

$$\int_{-\infty}^0\int_{-\infty}^0 \psi^*_{\sigma\sigma^*}\psi_{\sigma^*\sigma}\,dx\,dy = \text{INT} \tag{10.101}$$

Substituting equations (10.97)–(10.101) into equation (10.96) yields

$$\beta_{(\sigma\sigma^*)(\sigma^*\sigma)} = 0 \tag{10.102}$$

Therefore, if we move an H_2 molecule toward a D_2 in the configuration shown in Figure 10.39, there will be no coupling between the $\sigma\sigma^*$ and the $\sigma^*\sigma$ MOs. As a result, no reaction will occur. One can get some small amount of coupling if one distorts the geometry (e.g., by twisting the H_2 relative to the D_2). However, $\beta_{(\sigma\sigma^*)(\sigma^*\sigma)}$ is always small. As a result, one does not get a significant reaction.

Now it is useful to go back and consider why the picture of the transition state in Figure 10.37 was wrong. In Figure 10.37, we assumed that it will be possible to simultaneously break a H–H bond and form a H–D bond. However, if we multiply out all of the wavefunctions, we will find that during the reaction, we need to transform wavefunctions that look like $\phi_1\bar{\phi}_2\phi_3\bar{\phi}_4$ into wavefunctions that look like $\phi_1\bar{\phi}_2\bar{\phi}_3\phi_4$, where ϕ_1, ϕ_2, ϕ_3, and ϕ_4 are the atomic orbitals on atoms 1, 2, 3 and 4 (e.g., the two hydrogen atoms and the two deuterium atoms, respectively) and the bars represent spins. Physically, when we try to share an electron between the two states, as we would do if there were partial H–H bond and a partial H–D bond, we would find that we need a single electron to spinup and down at the same time. The electron cannot be both spinup and spindown simultaneously. Therefore, it is impossible to simultaneously break the H–H bond and form a H–D bond. That explains why Conroy and Malli (1969) found that the four-centered reaction has an activation energy of 515 kJ/mol.

Another way to get the same result is to go back to the stick model of the four-centered reaction in Figure 10.41. In the stick model, one is saying that in the transition state for the reaction, there are four σ bonds in the system with four total electrons. According to MO theory, the only way for the four-centered bonding to be stable would be for the four-centered bond to be one of eigenstates of the system. However, the eigenstates of the system are the four states shown in Figure 10.41. Of those, only the $\sigma\sigma$ state is bonding in both directions. One can put two electrons in the $\sigma\sigma$ state, but the other two electrons must be put into other molecular orbitals. These other MO are antibonding orbitals. As a result, the four-centered bonding in Figure 10.41 is not an eigenstate of the system. Therefore, quantum-mechanically, the four-centered bonding cannot occur.

A more subtle analysis shows that the reaction

$$H_2^+ + D_2^+ \longrightarrow \begin{bmatrix} H{-}H \\ | \quad | \\ D{-}D \end{bmatrix}^+ \longrightarrow 2HD^+ \tag{10.103}$$

where H_2^+ and D_2^+ are positively charged molecules, is allowed. However, in reaction (10.103) there are only two electrons in the transition state. One can put both electrons in the SS state so that the bonding is possible.

This example illustrates an important feature of Woodward and Hoffmann's analysis: There are many simple reactions that look plausable on paper but cannot occur because they involve bonding schemes that are not possible quantum-mechanically. We can draw a stick diagram like that in Figure 10.39 for many proposed transition states. However, there is no guarantee that the bonding shown in the stick diagram is possible. If it is not, the proposed reaction will have a very high activation barrier. Hence, one has to do some analysis before one assumes that one can get a proposed reaction to occur. A generalization of the analysis above shows that four-center reactions of species with σ

bonds are usually symmetry-forbidden. (There are exceptions where a nonbonding orbital can change the symmetry of the system.) Therefore, one would rarely expect to see four-centered reactions experimentally.

10.12 CONSERVATION OF ORBITAL SYMMETRY

One can imagine repeating the analysis in the last section for a series of reactions. One could simply work out all of the integrals. However, Woodward and Hoffmann found a trick that simplifies the analysis. The trick comes from group theory. Recall from Chapter 2 that we can classify surface structures based on the symmetry elements in the surface. In the same way, we can classify reaction paths in terms of their symmetry elements. For example, if we assume that hydrogen and deuterium are equivalent in the reaction in Figure 10.39 then the reaction coordinate has three mirror planes: the two lines indicated in the figure and the plane of the paper. There also are three 2-fold axes: two at the plane of the paper at the mirror planes and one perpendicular to the plane of the paper at the dot. The dot is also an inversion center. In a similar way, one can classify the symmetry of all of the MO of the system. Woodward and Hoffmann (1970) show that the symmetry of the MO determines whether a reaction can occur. If orbital symmetry is conserved, the coupling constants will be nonzero as the reaction can occur. However, if the orbital symmetry is not conserved, no reaction can occur.

10.12.1 Some Results from GroupTheory

We need to review some group theory to see how this idea arises. Recall that in group theory, one classifies the symmetry of molecules and the reaction pathways in terms of their point group. In Chapter 2, we noted that there are only 13 three-dimensional Bravis lattices and three space groups. In the same way, there are only 47 important point groups. There are more point groups than space groups because one can have 5-, 7-, 8-,. . ., fold axis in molecules, but not in a repeating three-dimensional (3D) structure. Cotton (1971) provides an excellent overview of the application of group theory to molecules and reactions, and there is no room to discuss all of the important ideas here. However, the key feature of the analysis is that if one knows the symmetry elements in a molecule or reaction path, one can use the tables in Cotton (1971) to find the point group.

The most important tables in Cotton's book are the character tables near the end of the book. The character tables include a listing of all of the important point groups and their symmetry elements. For example, Table 10.2 is a character table for the D_{2h} point group. The D_{2h} point group has three perpendicular 2-fold axes, three mirror planes, an inversion center, and an identity element (i.e., an element that does not change anything). Note that the transition state in Figure 10.39 has all of these symmetry elements and no extras. Therefore, we say that the reaction in Figure 10.39 follows the D_{2h} point group.

The character table also lists something called the **irreducible representations** of the point group. The idea of a group representation is more subtle than there is room to discuss here. However, basically, if we solve the Schroedinger equation for a molecule (or transition state) that has a given symmetry, then we can classify the independent solutions as being a member of one of several irreducible representations. (The irreducible representations are just a way to classify the solution of the Schroedinger equation in terms of their symmetry properties.) Each independent MO of a system will belong to a single irreducible representation. Hence, one can classify the symmetry of MO in terms of their irreducible representations.

Table 10.2 A character table for the D_{2h} point group

Irreducible Representation	Symmetry Element: Identity	z 2-Fold Axis	y 2-Fold Axis	x 2-Fold Axis	Inversion Center	xy Mirror Plane	xz Mirror Plane	yz Mirror Plane	Rotations and Orbitals
A_g	1	1	1	1	1	1	1	1	x^2, y^2, z^2
B_{1g}	1	1	−1	−1	1	1	−1	−1	r_z, xy
B_{2g}	1	−1	1	−1	1	−1	1	−1	r_y, xz
B_{3g}	1	−1	−1	1	1	−1	−1	1	r_x, yz
A_u	1	1	1	1	−1	−1	−1	−1	
B_{1u}	1	1	−1	−1	−1	−1	1	1	z
B_{2u}	1	−1	1	−1	−1	1	−1	1	y
B_{3u}	1	−1	−1	1	−1	1	1	−1	x

Source: Adapted from Cotton (1971).

The character table makes it easy to find the irreducible representation for each MO. Notice all the ones and minus ones in the character table (Table 10.2). The ones and minus ones tell what happens when each of the symmetry operations of the point group acts on a given MO. For example, the xy mirror plane converts y to −y. If we look down the xy mirror plane column in Table 10.2, we find that B_{2u} irreducible representation has a character of −1. Therefore, $\Psi_{B_{2u}}$, the wavefunction of an MO of B_{2u} symmetry in the D_{2h} point group, will be converted to $-\Psi_{B_{2u}}$ when y is converted to y. One can therefore determine the irreducible representation of a given MO by examining how the symmetry elements in the system affect the given MO.

For example, consider $\Psi_{\sigma^*\sigma}$ in Figure 10.40. $\Psi_{\sigma^*\sigma}$ does not change when it is reflected around the xy or yz mirror plane (i.e., the plane of the paper and plane 2 in Figure 10.40, respectively). However, it switches signs when it is reflected around the xz mirror plane (i.e., plane 1 in Figure 10.40). Therefore, the irreducible representation of $\Psi_{\sigma^*\sigma}$ should have a 1 in the column for the xy or yz mirror planes and a −1 in the column for the xz mirror plane. Table 10.2 shows that only the B_{2u} irreducible representation has the correct symmetry. Therefore, we conclude that $\Psi_{\sigma^*\sigma}$ has B_{2u} symmetry. The reader may want to show that $\Psi_{\sigma\sigma}$ has A_g symmetry, $\Psi_{\sigma\sigma^*}$ has B_{3u} symmetry, and $\Psi_{\sigma^*\sigma}$ has B_{1g} symmetry.

Now it is useful to go back to our analysis of equation (10.96). Note that we used the symmetry of the various wavefunctions to show that $\beta_{(\sigma\sigma^*)(\sigma^*\sigma)}$ is zero. Note that we could have done the analysis directly from the character table. For example, if we start with INT from equation (10.97) and let y go to −y (i.e., reflect around the xz mirror plane), $\psi_{\sigma^*\sigma}$ does not change while $\psi_{\sigma\sigma^*}$ is converted into $-\psi_{\sigma\sigma^*}$, which is completely symmetric (i.e., a member of the A_g irreducible representation), so $\psi_{\sigma\sigma^*}$ does not change either. Therefore

$$\text{INT}' = (-1)(1)(1)\text{INT} \tag{10.104}$$

As a result, one could have arrived at the results in Section 10.11.1 directly from the character table without doing detailed analysis.

One can generalize this result to show that the coupling coefficients are always zero unless orbital symmetry is conserved. Consider transferring an electron from $\psi_{\sigma\sigma^*}$ to some other wavefunction ψ_x. The transfer coefficient for the transfer, β_x, is given by

$$\beta_x = \int \psi^*_{\sigma\sigma^*} \psi_x \, d\vec{\tau} \tag{10.105}$$

If we start with a wavefunction of B_{2u} symmetry such as $\psi_{\sigma\sigma^*}$ and multiply by $\mathcal{H}$, we will still end up with a function of B_{2u} symmetry, since $\mathcal{H}$ is totally symmetric. Now, if we multiply by ψ_x we will get a new function that we will call Ξ. One can show from something called the **great orthogonality theorem** that if Ξ changes sign under any of the group operations when we integrate over all space, half the integral will be positive and half will be negative. As a result, β_x will be zero. Notice that we can tell whether Ξ changes sign directly under all of the group operations from the character table. If the irreducible representation of ψ_x has ones in any of the places where the irreducible representation of $\psi_{\sigma\sigma^*}$ has minus ones, or if the irreducible representation of ψ_x has minus ones in any of the places where the irreducible representation of $\psi_{\sigma\sigma^*}$ has ones, Ξ the integral in equation (10.97) will switch signs under at least one of the symmetry operations of the D_{2h} space group. As a result, β_x will be zero. The only instance where β_x will not be zero is when the irreducible representations of ψ_x and $\psi_{\sigma\sigma^*}$ have ones and minus ones in just the same places in the character table. That happens only when ψ_x and $\psi_{\sigma\sigma^*}$ have the same orbital symmetry (i.e., are members of the same irreducible representation).

The conclusion for the analysis in the last paragraph is that during the reaction, we can convert one molecular orbital into another only when both orbitals are of the same symmetry (i.e., members of the same irreducible representation). As a result, orbital symmetry is conserved during concerted chemical reactions.

10.13 EXAMPLES OF SYMMETRY-ALLOWED AND SYMMETRY-FORBIDDEN REACTIONS

It is useful to use these ideas to make some predictions about chemical reactions. Clearly, the first example is the four-centered reaction in Figure 10.39. Notice that we start with electrons in A_g and B_{2u} molecular orbitals and end up with electrons in the A_g and B_{3u} molecular orbitals. The orbital symmetry changes during the reaction. Hence, the reaction is forbidden.

Now consider the reaction

$$H + D_2 \longrightarrow HD + D \tag{10.106}$$

where a hydrogen atom reacts with D_2. For the purpose of analysis, let's assume that the reaction occurs with the hydrogen atoms and the two deuterium atoms lying in a line.

Figures 10.20 and 10.21 show MO diagrams for the reaction. One starts with a symmetric orbital and an antisymmetric orbital at the start of the reaction, and ends up with orbitals of the same symmetry. Consequently, orbital symmetry is conserved during reaction (10.22).

Calculations indicate that the reaction in Figure 10.12 has an activation energy of 34 kJ/mol while the reaction in Figure 10.39 has an activation energy of 515 kJ/mol.

This example illustrates an important point: We need to look carefully at a reaction pathway before we decide whether a reaction is allowed or forbidden. Many reactions that look feasible on paper do not occur because of symmetry constraints. In particular, symmetric four-centered reactions are usually forbidden, so they are rarely seen. Physically, they have large barriers to reaction.

10.14 SUMMARY

In summary, then, the results in this chapter showed that activation barriers are associated with

- Bond stretching
- Orbital distortion
- Quantum effects

We have provided some qualitative models to explain the variations. We will quantify the effects in Chapter 11.

10.15 SOLVED EXAMPLES

Example 10.A Using the Marcus Equation to Estimate Barriers for Reactions One of the more intriguing applications of the Marcus equation is in predicting the barriers for reactions. The idea is to estimate E_a^0 for an identity reaction, and then use that information to predict barriers.

An identity reaction is a reaction where a group is exchanged on a carbon center:

$$X + R - X \longrightarrow X - R + X \tag{10.A.1}$$

where X could be a neutral species or a charged ligand. Notice that ΔH_r is zero for an identity reaction according to equation (10.23). Consequently, $E^0_{a,xx}$, the intrinsic barrier

$$E^0_{a,xx} = E_{a,xx} \tag{10.A.2}$$

where $E_{a,xx}$ is the activation barrier for reaction (10.A.1).

Marcus supposed that when you have a nonidentity reaction

$$X + R - Y \longrightarrow X - R + Y \tag{10.A.3}$$

One can estimate $E^0_{a,xy}$, the intrinsic barrier for reaction (10.A.3), from

$$E^0_{a,xy} = \tfrac{1}{2}(E^0_{a,xx} + E^0_{a,yy}) \tag{10.A.4}$$

where $E^0_{a,yy}$ is the intrinsic barrier for reaction (10.A.1) when X is replaced by Y. To see how this works, let us try to estimate the activation barrier for the reaction

$$H' + CH_2 = CHCH_2OH \longrightarrow CH_2 = CHCH_2H' + OH \tag{10.A.5}$$

Equation (10.A.5) is equivalent to equation (10.A.3) with $X = H'$ and $Y = OH''$. Lee et al. (1995a) calculated the activation energy for the reactions

$$OH' + CH_2CHCH_2OH \longrightarrow CH_2CHCH_2OH' + OH \tag{10.A.6}$$

$$H' + CH_2 = CHCH_3 \longrightarrow CH_2 = CHCH_2H' + H \tag{10.A.7}$$

If we measure energies relative to the bound complexes, reaction (10.A.6) has an activation barrier of 27.9 kcal/mol, while reaction (10.A.7) has an activation barrier of 55.1 kcal/mol.

According to equation (10.A.4)

$$E^0_{a,xy} = \tfrac{1}{2}(27.9 + 55.1) = 41.5 \text{ kcal/mol} \tag{10.A.8}$$

According to data in Lee et al, reaction (10.A.5) is 47 kcal/mol exothermic (i.e., $\Delta H_r = -47$). According to equation (10.33)

$$E_a = E_a^0\left(1 + \frac{\Delta H}{4E_a^0}\right)^2 = 41.5\left(1 + \frac{-47}{(4)(41.5)}\right)^2 = 21.3 \text{ kcal/mol} \tag{10.A.9}$$

By comparison the actual value is 17.3 kcal/mol.

10.16 SUGGESTIONS FOR FURTHER READING

The connections between thermodynamics and kinetics are discussed in:

A. Pross, *Theoretical and Physical Principles of Organic Reactivity*, Wiley, New York, 1995.

S. S. Shaik, H. B. Schlegel, and S. Wolfe, *Theoretical Aspects of Physical Organic Chemistry*, Wiley, New York, 1992.

The connection between orbital pictures and molecular forces is discussed in:

R. F. W. Bader, *Atoms in Molecules: A Quantum Theory*, Oxford University Press, Oxford, UK, 1994.

10.17 PROBLEMS

10.1 Define the following terms:

(a) Polanyi relationship
(b) Marcus equation
(c) Intrinsic activation barrier
(d) Transfer coefficient
(e) Marcus inverted region
(f) Pauli repulsion
(g) Configuration mixing diagram
(h) Configuration mixing model
(i) Correlation diagram
(j) Symmetry-forbidden reaction
(k) Avoided crossing
(l) Tight transition state
(m) Loose transition state

10.2 Why do activation barriers arise during chemical reactions? What are the key factors in determining whether a reaction is activated? Why are activation energies reduced for fairly exothermic reactions? What happens with very exothermic reactions? Why?

10.3 How do Pauli repulsions affect barriers to reactions? Would there be a barrier in the absence of Pauli repulsions? Explain.

10.4 Describe in your own words how orbitals change as reactions proceed. How do atom transfer processes occur? What extra forces occur when a methyl group is transferred?

10.5 Describe the Polanyi equation. How does it arise? What are the key assumptions in the derivation? When is the equation useful? When does it fail?

10.6 Describe the Marcus equation. How does it arise? What are the key assumptions in the derivation of the Marcus equation? When is the equation useful? When

does it fail? What are the advantages of the Marcus equation over the Polanyi relationship? When is the Marcus equation appropriate? When should you use the Blowers–Masel approximation instead?

10.7 Compare and contrast the Marcus equation, the Polanyi relationship, and the Blowers–Masel approximation. Be sure to consider the key features of the derivation and the predictions. Why does the Marcus equation predict parabolic behavior for very exothermic and endothermic reactions while the Blowers–Masel approximation predicts linear behavior? What are the key different assumptions of the two models?

10.8 The data in Figure 10.11 show nonlinear behavior with ΔH_r.

(a) The plot actually shows ln(k) versus ΔH_r. Show that if data in the figure followed the Polanyi relationship and the preexponential were constant, a plot of ln(k) versus ΔH_r should be linear.

(b) Use the Marcus equation to explain why the curve is nonlinear.

(c) Does the Blowers–Masel approximation predict any different trends?

10.9 What are the key physical forces that are represented by the intrinsic barrier?

(a) According to the Marcus equation, what variables affect the intrinsic barrier?

(b) According to the Blowers–Masel equation, what variables affect the intrinsic barrier?

(c) How would charge transfer prior to reaction affect the intrinsic barrier?

(d) How would steric repulsions affect the intrinsic barrier?

10.10 Explain the key trends you see in the data in Figure 10.29. Why is there so much variability in the points? (*Hint*: look at the Blowers–Masel approximation and equation (10.11)—what varies as you change reactions?)

10.11 Compare the behaviors in Figures 10.17 and 10.18. Why do you see inverted behavior in Figure 10.17 but not in Figure 10.18?

10.12 In your organic chemistry class you learned about steric effects in reactions.

(a) How do the steric interactions affect the Blowers–Masel approximation?

(b) How does the tightness of the transition state change as the steric interactions change?

(c) How will your results in (b) affect the predictions of the Polanyi relationship?

(d) How will your results in (b) affect the predictions of the Marcus equation?

10.13 The objective of this problem is to use what you learned in organic chemistry class to estimate the intrinsic barriers for a series of reactions of the form

$$HO + CHR_3 \longrightarrow H_2O + CR_3$$

(a) How would the C–H bond energy change as you change the R group from H to CH_3 to $C(CH_3)_3$.

(b) How will the Pauli repulsions change? (Hint: How does the size of the electron clouds change?)

(c) Will the barrier go up or down?

(d) How would an electron-withdrawing group affect the intrinsic barrier?

Table P10.14 Preexponentials and activation barriers for the reaction NH + H–R → NH_2 + R

R	E_a, kcal/mol	k_0, cm^3(mol·second)	R	E_a kcal/mol	k_0 cm^3(mol·second)
CH_3	20	9×10^{13}	$CH(CH_3)_2$	14.5	6×10^{13}
CH_2CH_3	16.5	7×10^{13}	$(CH_3)_2CO$	11.5	5×10^{13}

Source: Data of Rhorig and Wagner, Berichte Bunsen Gesellschaft Physik. Chem. 98, 858 (1994)

10.14 Rhorig and Wagner, Berichte Bunsen Gesellschaft Physik. Chem. **98**, 858 (1994) examined a number of hydrogen abstraction reactions of the form

$$NH + H\text{–}R \longrightarrow NH_2 + R$$

Their data are given in Table P10.14.

(a) Use data in the CRC and the NIST Webbook to estimate the heat of reaction for each of the reactions in the table.

(b) Fit the data to a Polanyi plot. How well do they fit?

(c) Try fitting the data to the Marcus equation. Assume that the intrinsic barrier is constant. How well do the data fit?

(d) Does the assumption that the intrinsic barrier is constant make sense, or should the intrinsic barrier vary? (*Hint*: Look at what determines an intrinsic barrier.)

(e) Examine the variations in the preexponential. According to transition state theory, is the tightness of the transition state changing?

(f) Use the data in Table P10.14 to estimate the role of the tightening of the transition state in raising or lowering the intrinsic barrier. Should the intrinsic barrier go up or down?

(g) Try fitting the data to the Blowers–Masel equation. Assume that the V_P is constant. How well do the data fit?

(h) Does the assumption that the V_P is constant make sense, or should V_P vary and instead the intrinsic barrier be constant?

10.15 Maslack, Vallombroso, Chapman, and Narvaez, Angew. Chem. 33 (1994) examined the rate constant for a number of bond cleavage reactions. Their data are given in Table P10.15.

(a) Maslack et al. showed that ln(k) versus ΔH_r is nonlinear. Show that if data followed the Polanyi relationship and the preexponential were constant, a plot of ln(k) versus ΔH_r should be linear.

(b) Use the Marcus equation to explain why the curve is nonlinear.

(c) How well does the Marcus equation fit the data?

(d) Does the Blowers–Masel approximation predict any different trends?

(e) How well does the Blowers–Masel approximation fit the data?

(f) Try adjusting the temperature in the fit; do you get a better fit?

(g) What do you conclude from the fact that you need to adjust the temperature?

Table P10.15 Rate constants at 300 K and heats of reaction for the series of reactions considered by Maslack, Vallombroso, Chapman, and Narvaez, Angew. Chem. 33 (1994)

Reaction number	ln(k), cm^3/(mol·second)	H_r, kcal/mol	Reaction Number	ln(k), cm^3/(mol·second)	H_r, kcal/mol
(1c)	−7.4	24.8	(3a)	5.9	5.7
(1d)	−7.0	23.9	(3b)	7.0	2.8
(1e)	−4.7	18.7	(3c)	8.6	−1
(1f)	−3.2	18.2	(3d)	9.6	−12.3
(1g)	−2.5	16.3	(3e)	10.5	−17.6
(1h)	−2.7	15.9	(4a)	8.8	4.6
(2a)	−0.2	15.2	(4b)	9.1	4
(2b)	0.7	14.5	(4c)	9.6	3
(2c)	1.3	13.2	(4d)	6.4	3.9
(2d)	1.6	13.2	(4e)	7.4	4.8
(2e)	1.8	10.7	(5)	0.2	15.6
(2f)	5.2	7.8	—	—	—
(2g)	5.7	6.6	—	—	—
(2h)	5.6	6.2	—	—	—

10.16 Lee, Kim and Lee, J. Computational Chem. 16 (1995b) examined the activation energy for a number of allyl transfer reactions:

$$X^- + CH_2{=}CHCH_2Y \longrightarrow CH_2{=}CHCH_2X + Y^-$$

Table P10.16 shows a selection of their results

(a) Fit the data to a Polanyi plot. How well do they fit?

(b) Try fitting the data to the Marcus equation. Assume that the intrinsic barrier is constant. How well do the data fit?

(c) Does the assumption that the intrinsic barrier is constant make sense, or should the intrinsic barrier vary? (*Hint*: Use the additivity assumption to estimate the barriers.)

Table P10.16 Activation energy for a number of allyl transfer reactions

X	Y	ΔH_r, kcal/mol	E_a, kcal/mol	X	Y	ΔH_r, kcal/mol	E_a, kcal/mol
H	H	0	55.1	F	H	+67.2	74.4
NH_2	NH_2	0	43.3	OH	H	+47.1	64.3
OH	OH	0	27.9	NH_2	H	+26.1	59.2
F	F	0	15.0	Cl	H	+87.5	92.2
PH_2	PH_2	0	33.3	SH	H	+67.3	77.6
SH	SH	0	24.9	PH_2	H	+47.2	67.4
Cl	Cl	0	18.8	OH	F	−16.1	13.1
OH	Cl	−38.9	5.6	NH_2	F	−40.7	5.8
NH_2	Cl	−60.1	3.5	Cl	F	+16.9	32.7
SH	Cl	−19.8	13.45	SH	F	+0.4	22.0
PH_2	Cl	−41.1	7.28	PH_2	F	−20.4	15.0

Source: Results of Lee, Kim and Lee, *J. Computational Chem.* **16** (1995) 1045.

(d) Try fitting the data to the Blowers–Masel equation. Assume that the V_P is constant. How well do the data fit?

(e) Does the assumption that the V_P is constant make sense, or should V_P vary and instead E_A^0 be constant?

(f) Use the methods in Example 10.A to estimate the barriers to all of the reactions. How well does the method work?

10.17 Bernasconi and Ni (1994) describe two different methods to estimate the intrinsic barriers for a series of reactions of the form

$$X^- + HX \longrightarrow XH + X^- \qquad \text{(P10.17.1)}$$

They were not able to measure the intrinsic barriers directly, but they were able to get an indirect measure by examining relative rates of reactions. The results are given in Table P10.17. The question is how you can do an experiment to see which measure of the intrinsic barrier is accurate. By way of background, nonidentity proton exchange experiments

$$X^- + HY \longrightarrow XH + Y^- \qquad \text{(P10.17.2)}$$

can easily be done, so the object is to find a way to use an exchange reaction to distinguish between the two measures of intrinsic barriers.

(a) How many nonidentity reactions can you form from the X groups in Table P10.17?

(b) Use Marcus' additivity postulate to estimate the intrinsic barriers for each of these nonidentity reactions.

(c) Which nonidentity reaction will show the largest differences?

(d) Look in Bernasconi and Ni's paper and find data for that reaction.

(e) Which measure of the intrinsic barrier fits best?

10.18 Consider the following series of reactions:

$$HO + CH_4 \longrightarrow H_2O + CH_3$$

$$HO + CH_3CH_3 \longrightarrow H_2O + CH_2CH_3$$

Table P10.17 Intrinsic barriers for a number of reactions of the form $X^- + HX \rightarrow XH + X^-$

X	E_a^0, kcal/mol Estimated Using an Amine Reference, kcal/mol	E_a^0, kcal/mol Estimated Using a 9-Cyanofluorene Reference, kcal/mol
$[(CH_3)NH_2]^+$	6.80	9.37
Benzylmaloniumnitrite	11.52	13.87
9-Cyanofluorene	15.40	13.05
1,3-Indandione	16.72	14.37
4-Nitrophenylacetonitrite	17.62	15.17
(3-Nitrophenyl)nitromethane	21.74	19.39
(4-Nitrophenyl)nitromethane	21.96	19.61
Phenylnitromethane	22.64	20.17

$$HO + CH_2(CH_3)_2 \longrightarrow H_2O + CH(CH_3)_2$$

$$HO + CH(CH_3)_3 \longrightarrow H_2O + C(CH_3)_3$$

(a) Use Benson's approximation from Chapter 6 to estimate the heat of reaction for each of the reactions and the energies of the bonds that form and break.

(b) Estimate the strength of the Pauli repulsions, assuming that the hydrogen–methyl potential is given by

$$V_r = (1.5 \text{ kcal/mol}) \exp\left(\frac{4.5 \text{ Å} - R_{O\text{-}H}}{0.75 \text{ Å}}\right)$$

Be sure to consider that in the reaction $H + CH_2(CH_3)_2 \rightarrow H_2 + CH(CH_3)_2$ the incoming hydrogen is in close proximity to three methyl groups.

(c) Use the Blowers–Masel approximation to estimate the barriers for the reaction.

(d) Make a Polanyi plot of the data and estimate the intrinsic activation barrier and transfer coefficient.

(e) Why is the transfer coefficient negative?

(f) Does the derivation of the Polanyi relationship allow the transfer coefficient to be negative?

(g) Does the Marcus equation allow the transfer coefficient to be negative?

10.19 Why are there orbital symmetry barriers to reaction? Where do they arise, and where are they important? How does the orbital symmetry barrier affect the reaction $H_2 + D_2 \rightarrow 2HD$? What would the orbital diagrams look like for a symmetry-forbidden reaction?

10.20 **(a)** Show mathematically that the four-centered reaction $A_2 + B_2 \rightarrow 2AB$ is symmetry-forbidden.

(b) What is the physical significance of this result? (*Hint*: Show that in the four-centered configuration, it is impossible to simultaneously have an A–A, B–B, and two A–B bonds.)

10.21 Lopes et al. (1999) examined the role of acyloxymethyl as a way to protect antibiotics from degradation (hydrolysis) by bacteria.

(a) Read the paper and report on the findings

(b) The Brønsted plot is curved. How do Lopes et al explain the curvature?

(c) Could the curvature be due the a shift in the position of the transition state as suggested from the Marcus formulation?

10.22 Consider the reaction $D + H_2 \rightarrow HD + H$. Figures 10.20 and 10.21 show diagrams of the key orbitals during the reaction.

(a) The pictures only show states that would be expected to be occupied. What will the empty states look like? (*Hint*: In the empty states, bonding orbitals are converted to antibonding orbitals.)

(b) Draw a configuration mixing diagram during the reaction. (*Hint*: The configuration mixing diagram links up MOs in the ground state of reactants with MOs with the same pattern of plusses and minuses in the excited states of the products and vice versa.)

(c) Do the orbitals really follow the configuration mixing diagram? Specifically can you see the excited state being mixed into the ground state?

(d) Are there any extra interactions not considered in the configuration mixing diagram?

(e) Draw a correlation diagram for the system. (*Hint*: The correlation diagram links up MOs in the ground state of the reactants with MOs with the same pattern of plusses and minuses in the products.)

(f) Do the orbitals really follow the configuration mixing diagram? In other words, can you see a continuous transition from reactants to products?

(g) Are there any extra interactions not considered in the configuration mixing diagram?

More Advanced Problems

10.23 Roberts and Steele J. Chem. Soc., Perkin Trans. 2, (1994), fit the activation barriers for a number of atom transfer reactions to a complex expression.

(a) Read Roberts and Steele's paper and explain why all of the factors arise.

(b) Relate the findings to the Blowers–Masel model. How are the variations in the Pauli repulsions considered in the Roberts–Steele model?

(c) Are there any factors in the Roberts–Steele model that are ignored in Blowers–Masel's model?

10.24 Zavitsas J. Chem. Soc., Perkin Trans. 3, (1998), refit the activation barriers for a number of atom transfer reactions.

(a) Read Zavitsas paper and explain why all of the factors arise.

(b) How does Zavitsas model compare to that of Roberts and Steele J. Chem. Soc., Perkin Trans. 2, (1994)?

(c) Relate the findings to the Blowers–Masel model. How are the variations in the Pauli repulsions considered in Zavitsas model?

(d) Are there any factors in Zavitsas model that are ignored in the Blowers–Masel model?